

**GA-A23344**

# **DIII-D LONG RANGE PLAN**

**by  
DIII-D RESEARCH STAFF**

**FEBRUARY 2000**

## **DISCLAIMER**

This report was prepared as an account of work sponsored by an agency of the United States Government. Neither the United States Government nor any agency thereof, nor any of their employees, makes any warranty, express or implied, or assumes any legal liability or responsibility for the accuracy, completeness, or usefulness of any information, apparatus, product, or process disclosed, or represents that its use would not infringe privately owned rights. Reference herein to any specific commercial product, process, or service by trade name, trademark, manufacturer, or otherwise, does not necessarily constitute or imply its endorsement, recommendation, or favoring by the United States Government or any agency thereof. The views and opinions of authors expressed herein do not necessarily state or reflect those of the United States Government or any agency thereof.

**GA-A23344**

# **DIII-D LONG RANGE PLAN**

**by  
DIII-D RESEARCH STAFF**

**Work supported by  
the U.S. Department of Energy  
under Contract No. DE-AC03-99ER54463**

**GA PROJECT 30033  
FEBRUARY 2000**

## APPROVALS

Approved:

\_\_\_\_\_  
R.D. Stambaugh  
DIII-D Program Director  
General Atomics

\_\_\_\_\_  
Date

\_\_\_\_\_  
M.S. Foster  
Onsite Technical Representative  
Berkeley Site Office  
DOE/OAK

\_\_\_\_\_  
Date

\_\_\_\_\_  
W. Marton  
Facility Operations Manager  
DOE Office of Fusion Energy Science

\_\_\_\_\_  
Date

\_\_\_\_\_  
E. Oktay  
DIII-D Program Manager  
DOE Office of Fusion Energy Science

\_\_\_\_\_  
Date

## DIII-D RESEARCH COUNCIL

July 1999 to July 2000

R. Stambaugh (Chair)

J. deGrassie (Experiment Coordinator)

### **At-Large Members**

J. DeBoo (GA)  
R. Groebner (GA)  
C. Greenfield (GA)  
L. Johnson (PPPL)  
L. Lao (GA)  
R. Moyer (UCSD)  
M. Murakami (ORNL)  
R. Perkins (PPPL)  
C. Petty (GA)  
P. Politzer (GA)  
C. Rettig (UCLA)  
A. Turnbull (GA)  
R. Waltz (GA)  
P. West (GA)

### **Thrust Leaders**

E. Doyle (UCLA)  
J. Ferron (GA)  
A. Garofalo (Columbia U)  
R. La Haye (GA)  
J. Lohr (GA)  
T. Luce (GA)  
M.A. Mahdavi (GA)  
J. Navratil (Columbia U)  
M. Okabayashi (PPPL)  
E. Synakowski (PPPL)  
M. Wade (ORNL)

### **Standing Members**

S. Allen (LLNL)  
D. Baldwin (GA)  
K. Burrell (GA)  
V. Chan (GA)  
R. Callis (GA)  
A. Hyatt (GA)  
A. Kellman (GA)  
J. Luxon (GA)  
P. Petersen (GA)  
R. Prater (GA)  
D. Schissel (GA)  
R. Snider (GA)  
E. Strait (GA)  
T. Taylor (GA)  
T. Simonen (GA)

## **DIII-D PROGRAM ADVISORY COMMITTEE MEMBERS (Meeting: January 20–21, 2000)**

Prof. Charles Baker (UCSD)

Prof. James Drake (U. Maryland)

Dr. Richard Hawryluk (PPPL)

Dr. Shigeru Konoshima (JAERI, Japan)

Dr. William M. Nevins (LLNL)

Prof. George Vlasses (U. Washington)

Dr. Steven Wolfe (MIT)

Dr. Jill Dahlburg (NRL)

Prof. Raymond Fonck (U. Wisconsin)

Prof. Richard Hazeltine (U. Texas)

Prof. Sergei Krasheninnikov (USCS)

Dr. Martin Peng (ORNL)

Dr. Michael Watkins (JET, Europe)

Prof. Hartmut Zohm (MPI, Garching)

## FOREWORD

This document describes the long-range plan for the DIII-D National Program which is updated annually and forms the background for the DIII-D annual experiment plan and the budget submittals to the U.S. Department of Energy.

The DIII-D long range program plan supports the Fusion Energy Sciences Program mission of advancing fusion science and fusion technology; to establish the knowledge base for an economically attractive energy source for the nation and the world. The unique capabilities of DIII-D are used in an innovative program of understanding and demonstrating the potential of tokamak improvement. This program plan strongly emphasizes the study of fusion plasma physics (stability, transport, wave/particle interactions and plasma wall interactions) in an integrated manner that aids in developing understanding of other toroidal magnetic concepts.

The integrated goal of this research program is to demonstrate good high-beta plasma confinement with utilizing rf current drive and particle control to sustain and optimize the bootstrap-driven non-inductive advanced tokamak configuration. Success in DIII-D will provide the database for an improved tokamak (steady state, low-disruptivity, and compact) that would help speed the commercialization of magnetic fusion energy.

This program is carried out with extensive national collaboration at the flexible DIII-D tokamak facility. Principal among GA's collaborators are the on-going cooperative efforts with the Japan Atomic Energy Research Institute (JAERI), the Lawrence Livermore National Laboratory (LLNL), Oak Ridge National Laboratory (ORNL), Princeton Plasma Physics Laboratory (PPPL), University of California at Los Angeles and San Diego (UCLA and UCSD), and Sandia National Laboratory (SNL). On-site university collaborators include: Columbia University; Massachusetts Institute of Technology (MIT); the University of Maryland, the University of California at San Diego, Los Angeles, and University of California at Irvine; University of Texas; University of Wisconsin; and Hampton University. In addition, the DIII-D program continues to provide facilities for training graduate students and post doctoral fellows. Foreign laboratory groups involved in cooperative programs on DIII-D include the Joint European Tokamak (JET); Culham Laboratory; Max-Planck-Institute für Plasmaphysik, Garching; Institute for Plasmaphysics KFA, Jülich; Centre d'Etudes Nucleaires de Cadarache; Kurchatov Institute of Atomic Energy, Moscow; Troitsk Institute for Development of Thermonuclear Research; Korean Basic Science Institute; and Korean Advanced Institute of Science and Technology. In addition to hosting scientists to

participate in DIII-D experiments, DIII-D scientists participate in experiments at other laboratories.

The DIII-D program plan was developed as an outgrowth of feedback and input received on the draft plan developed by the DIII-D Executive Committee that was discussed at the DIII-D National Workshop attended by approximately 180 scientists on July 8-10, 1997. Following the National workshop the DIII-D Executive Committee developed a further prioritized program that was reviewed by the DIII-D Program Advisory Committee on February 3-4, 1998. With subsequent changes, GA submitted a five-year proposal which was peer reviewed on June 2-4, 1998. With appropriate modifications, this became the DIII-D Long Range Plan.

The year 2000 DIII-D Long Range Plan follows closely the 1999 version but incorporates input resulting from a two week community meeting in Snowmass, Colorado July 11-23, 1999, and from the FESAC Panel Report on Priorities and Balance of August 18-21, 1999. The Year 2000 plan was reviewed with the DIII-D Program Advisory Committee on January 20-21, 2000.

To carry out research described in this plan requires the support of the national research team, facility operations, and facility upgrades. The overall DIII-D funding for GA and collaborative institutions in FY00 is \$54.1M (Science \$23.0M, Facility Operations \$25.0M, and Capital and Upgrades \$6.1M).

Upgrades of DIII-D are underway to move toward the particle control and current profile control to enable DIII-D to carry out the intermediate pulse length research on the Advanced Tokamak called for in the recent FESAC document on five year goals for fusion research. Those upgrades are nearing completion as indicated by the table below. This Long Range Plan assumes that as these facility upgrades are completed, needed funding will be provided for a full implementation of the current profile control systems and other facility modernization and refurbishment projects. Further increases in future funding would allow increased facility operating time for deeper scientific investigations and to increase the number of experiments being carried out. Overall, this Long Range Plan enables the Fusion Energy Sciences Program to obtain maximum scientific productivity from the DIII-D Program.



**January 2000 Upgrade Plan (\$M)**

<b>Subsystem</b>	<b>FY92</b>	<b>FY93</b>	<b>FY94</b>	<b>FY95</b>	<b>FY96</b>	<b>FY97</b>	<b>FY98</b>	<b>FY99</b>	<b>FY00</b>	<b>FY01</b>	<b>Total</b>
Radiative Divertor	–	–	–	1.2	2.1	1.5	0.6	1.6	0.3	–	7.3
ICRF Power Upgrade	0.3	2.4	4.5	0.2	0.3	–	–	–	–	–	7.7
ECRF Power Upgrade	–	–	0.1	2.0	0.9	0.4	0.6	2.4	4.5	1.5	12.4
<b>Total</b>	<b>0.3</b>	<b>2.4</b>	<b>4.6</b>	<b>3.4</b>	<b>3.3</b>	<b>1.9</b>	<b>1.2</b>	<b>4.0</b>	<b>4.8</b>	<b>1.5</b>	<b>27.4</b>

Later Upgrades

TBD

In summary, this DIII-D program is aligned with the 1999 FESAC recommendation for priority emphasis on developing fusion science understanding and demonstrating tokamak improvement aimed at steady-state reduced-disruptivity high power density tokamak operation. Advanced tokamak results from 1999 provide confidence that the DIII-D program objective (to carry out an integrated long-pulse demonstration of a well-confined high-beta plasma with noninductive current drive) can be carried out in an advanced tokamak operating mode which reduces the plasma current needed, and is attractive for future tokamak steady-state operation.

# 1. EXECUTIVE SUMMARY

## 1.1. MISSION OF THE DIII-D NATIONAL FUSION PROGRAM

The overall mission statement of the DIII-D Program is “To establish the scientific basis for the optimization of the tokamak approach to fusion energy production.”

The main output of the DIII-D Research Program is a scientific basis. “Scientific” means developing a solid understanding of the underlying physical principles and incorporating it into useful predictive modeling tools. “Optimization” means experimentally demonstrating performance parameters at the theoretically predicted limits for the tokamak magnetic confinement system and achieving to the greatest degree possible an integrated, steady-state demonstration of optimized performance that projects to an attractive fusion power system. The integrated optimization sought and the scientific basis established will allow the definition of optimal paths to fusion energy using the tokamak approach.

## 1.2. DIII-D NATIONAL PROGRAM RESEARCH GOALS

This mission has been elaborated by the DIII-D Research Council in three additional research goal statements.

1. The DIII-D Program's primary focus is the Advanced Tokamak (AT) Thrust that seeks to find the ultimate potential of the tokamak as a magnetic confinement system.
2. Where it has unique capabilities, the DIII-D Program will undertake the resolution of key enabling issues for advancing various magnetic fusion concepts.
3. The DIII-D Program will advance the science of magnetic confinement on a broad front, utilizing its extensive facility and national team research capability.

Determining the ultimate potential of the tokamak as a confinement system is a complex scientific endeavor. The integration of advanced tokamak elements into achievable single discharges requires programmatic compromise and tradeoffs evolved over a multi-year period.

In order to provide more focus on critical issues in the DIII-D Program, the method of organization of the experimental research was changed in 1998. The main motivation for the new scheme was the desire to gain a more purposeful and visible path to the eventual AT integrated plasma scenarios targeted in the Five-Year Plan. This new scheme also makes it natural to create cross-disciplinary teams to pursue integrated

plasma scenarios. The new scheme is a matrix type of approach in which one dimension of the matrix is a set of Thrusts. A Thrust is aimed at a key objective of the research and is given a significant block of run time in which to realize its objectives. The research thrusts and their leaders will change year-to-year to keep up with the evolution of the experimental program. Most of the thrusts in the 2000 run plan relate to the AT goal of the DIII-D Program. The AT Program in its broad outlines is described in Section 2.2 of the Five-Year Plan. This work pursues Goal 1 above.

The second dimension of the experimental planning matrix is comprised of the four enduring topical areas of fusion energy science: stability, confinement and transport, divertor/edge physics, and heating and current drive. The DIII-D Facility and the DIII-D National Team is a resource of immense value to the U.S. Fusion Program in terms of advancing the science of magnetic confinement on a broad front. DIII-D has a superb diagnostic set, increasingly flexible and capable plasma control systems, an excellent research staff, and a comprehensive set of analysis codes and theory support that enable real learning in depth from the experiments done. The staff recognizes and embraces a responsibility to the greatest extent possible to use that resource to advance the state of fusion energy science knowledge generally.

The managers of these topical areas implement this second dimension of the matrix and have responsibility for the work supporting Goal 3 above. Their continuing leadership of these topical areas over a period of years assures the continued scientific focus of the DIII-D research. A thorough discussion of the scientific topics being pursued in the DIII-D Program can be found in Section 2.3 in the Five-Year Plan.

The DIII-D Research Staff also are strongly motivated to see magnetic confinement progress to future next-step devices. The AT work and the broader scientific work on DIII-D can contribute greatly to the definition and the support for these future machine initiatives. Some of those possible next step options are:

- An international D-T burning plasma experiment such as the RTO-RC ITER which plans more exploitation of and/or reliance on AT physics.

- An advanced performance superconducting tokamak (JT-60SU, ARIES-RS) which exploits AT physics toward steady-state.

- A copper-coil ignition experiment about the size of JET and using gyroBohm scaling of H-mode, relying on more conventional tokamak physics.

- A compact, high magnetic field copper-coil ignition experiment (as exemplified by CIT/BPX/IGNITOR) but enabling studies of or relying on AT physics (FIRE).

- A next-step spherical torus which relies on most elements of AT physics to enable the study of burning plasma physics in long pulse or steady-state.

Research toward Goal 2 can appear either as thrusts or as elements of the Topical Science Area plans. A discussion of how DIII-D research relates to the various future machine possibilities can be found in Section 2.4 of the Five-Year Plan.

Competition for experimental time on DIII-D is intense. Priority goes to the Advanced Tokamak work, which occupies most of the thrusts. We seek to reserve about 30%–40% of the run time for the Topical Area Managers to allocate to more broadly motivated studies. The work to support Goal 2 has to find time either as a thrust or in the Topical Areas.

### 1.3. DIII-D AND FESAC FIVE-YEAR GOALS

In this section, we outline how in the next five years the DIII-D National Program will make major contributions to the newly defined FESAC Goals and Objectives for Magnetic Fusion Energy (see Table 1: Goals and Near-Term/Long-Term Objectives for MFE, "Report of the FESAC Panel on Priorities and Balance," September 1999).

#### FESAC Goal 1

Goal: • Advance fundamental understanding of plasma, the fourth state of matter, and enhance predictive capabilities, through comparison of experiments, theory and simulation.

In the area of high temperature plasma science the DIII-D combines an internationally unexcelled capability for reproducibly producing high temperature plasmas in a wide range of plasma shapes, a unique ensemble of plasma diagnostics with outstanding spatial and temporal resolution, and close coupling to the exceptional U.S. MFE theory and modeling community. The FESAC 5-year objectives and specific DIII-D 5-year research directions are:

- **Turbulence and Transport:** *Advance understanding of turbulent transport to the level where theoretical predictions are viewed as more reliable than empirical scaling in the best understood systems.*

An overall goal for the DIII-D program is to work towards a predictive understanding of tokamak transport. Achieving this goal requires the combined efforts of theorists, modelers, and experimentalists to develop the fundamental theories, include them in numerical models, compare those models with the results of experiments and then iteratively improve them. The key issues here are understanding turbulent transport in both the electron and ion channels. Our work over the next few years will include fundamental investigations of the

nature of tokamak turbulence, comparison of those turbulence measurements with predictions of gyrokinetic and gyrofluid codes, and definitive tests of present-day transport models in well-diagnosed plasmas using both steady-state and modulated techniques. In addition, we will be further testing the model of  $E \times B$  shear suppression of turbulence by utilizing various techniques (e.g. impurity injection, electron heating) to investigate the functional dependence of the turbulence growth rates on these plasma parameters. Finally, by use of  $E \times B$  shear to stabilize the longer wavelength, ion temperature gradient modes, we will attempt to isolate and investigate the shorter wavelength modes which primarily affect electron transport.

- **Macroscopic Stability:** *Develop detailed predictive capability for macroscopic stability, including resistive and kinetic effects.*

DIII-D is conducting experiments aimed at validating theoretical models for ideal, resistive, and kinetic plasma instabilities using experimental measurements adequate for quantitative tests of the theoretical calculations. The goal is to extend the DIII-D performance to the theoretical limits of stability and to develop the intellectual, computational, and laboratory tools necessary to apply these results to other devices.

- **Wave-Particle Interactions:** *Develop predictive capability for plasma heating, flow and current drive, as well as energetic particle driven instabilities, in power-plant relevant regimes.*

The DIII-D Program will develop methods of plasma current generation (initiation, rampup, sustainment, and profile control) to provide future devices the basis for full steady-state transformerless operation. DIII-D is developing the physics basis being embodied in predictive codes for electron cyclotron, fast wave, and neutral beam current drive and for maximal use of the self-driven bootstrap current.

- **Multi-Phase Interfaces:** *Advance the capability to predict detailed multi-phase plasma-wall interfaces at very high power- and particle- fluxes.*

DIII-D will bring 2-D measurements of divertor plasma properties into comparison with 2-D predictive code calculations of those properties. The DIII-D principal research direction will be to maximize the degree of recombination and radiation in the divertor plasma in order to minimize heat fluxes to and erosion of plasma facing surfaces. Detached plasma states with high recombination fractions have been found and successfully simulated in the

2-D codes. The frontier task is to achieve these regimes in the lower density plasmas optimal for current drive and high bootstrap fractions.

## FESAC Goal 2

Goal: • *Resolve outstanding scientific issues and establish reduced-cost paths to more attractive fusion energy systems by investigating a broad range of innovative magnetic confinement configurations.*

The Advanced Tokamak vision of the ultimate potential of the tokamak as defined by theory work has extremely hollow current profiles and nearly 100% self-organized bootstrap current produced by high quality transport barriers near the plasma edge. These equilibria are certainly highly innovative and are so different from normal tokamak experience as to essentially constitute an alternate concept. Studies have shown that these modes, if realized, can halve the cost of electricity in tokamak fusion power systems.

The experimental and theoretical research DIII-D carries out in pursuit of the AT vision has many elements of generic value across magnetic confinement concepts:

- **Electrostatic Turbulence Suppression:** The mechanism of stabilization of at least electrostatic turbulence by sheared  $E \times B$  flows, pioneered by DIII-D, appears to be universal across magnetic confinement concepts and is a continuing focus of DIII-D research.
- **Wall Stabilization:** The physics and technology of stabilization of modes by a nearby conducting wall and feedback coil system being investigated on DIII-D is a development necessary for the spherical torus, RFP, spheromak, and FRC.
- **Energetic Particle Density Gradient Driven Instabilities:** The study of these instabilities was identified as having generic value across concepts at the Snowmass Summer Study. Such modes, excited by the fast ions from the neutral beams, are an important subject of study in DIII-D.
- **Current Drive by Waves and Beams:** The wave-particle and beam-plasma interaction physics, developed in the tokamak generally and DIII-D in particular, for driving current is largely generic across magnetic concepts.
- **Parallel Field Line Physics:** The physics investigations in the scrape-off layer and divertor plasmas is largely generic across concepts because of the dominant role of the parallel heat and particle flows and the prominence of concept non-specific atomic physics. The DIII-D divertor research emphasis on systematic

experiments, 2-D diagnostic measurements, and modeling enables transfer to other concepts of the understanding gained.

### FESAC Goal 3

Goal: • *Advance understanding and innovation in high-performance plasmas, optimizing for projected power-plant requirements; and participate in a burning plasma experiment.*

The DIII-D National Program was instrumental in defining the Advanced Tokamak concept. This vision of the ultimate potential of the tokamak as defined by theory work has extremely hollow current profiles and nearly 100% self-driven bootstrap current produced by high quality transport barriers near the plasma edge. Theory predicts that with wall stabilization of ideal modes the beta limit in the tokamak can be about twice the free boundary limit. Transport rates as low as neoclassical in the ions are envisioned and have been seen in experiments. Detached, highly recombining divertor operation needs to be combined with these advanced core plasma modes. Studies have shown that these modes, if realized, can halve the cost of electricity in tokamak fusion power systems and enable modest sized burning plasma experiments reaching for high gain and steady-state.

The FESAC 5-year objectives and specific DIII-D 5-year research directions are:

- *Assess profile control methods for efficient current sustainment and confinement enhancement in the Advanced Tokamak, consistent with efficient divertor operation, for pulse length  $\gg \tau_E$ .*

Efficient current sustainment will be achieved on DIII-D by maximizing the bootstrap current and supplementing that with electron cyclotron, fast wave, and neutral beam current drive. Near term scenarios being pursued aim at bootstrap fractions over 50% and sustained with current profile control (for up to 5 seconds) by microwave ECH power in a divertor plasma with a normalized beta of 4 and an energy confinement enhancement 2.5 times L-mode. Parallel lines of research on transport barrier physics and divertor physics in closed, pumped divertors are laying the groundwork for eventual long pulse integrated scenarios beyond the near term work.

- *Develop and assess high-beta instability feedback control methods and disruption control/amelioration in the Advanced Tokamak, for pulse length  $\gg \tau_E$ .*

DIII-D is developing the physics and the technology of stabilization of kink modes by a conducting wall backed by non-axisymmetric feedback coils.

Stabilization of neoclassical tearing modes by direct application of ECCD and indirect methods of current profile alteration by ECCD will be researched. DIII-D has an extensive program of stability studies and plasma control development aimed at enabling disruption free operation close to stability limits. The injection of impurity pellets, massive gas puffs, or liquid jets shows promise of success at providing a means of ameliorating the consequences of disruptions.

#### **FESAC Goal 4:**

Goal: • *Develop enabling technologies to advance fusion science; pursue innovative technologies and materials to improve the vision for fusion energy; and apply systems analysis to optimize fusion development.*

The DIII-D will deploy, and thereby foster, the development of a number of enabling and innovative technologies. Most notable are advanced methods for plasma heating and current drive (microwave ECRF); disruption mitigation by solid, liquid, or gas injection; plasma fueling (inside pellet launch); plasma flow control (neutral beam, ECRF, ICRF); investigation of novel divertor concepts; feedback technologies for wall stabilization; studies of surface erosion; and small-sample testing of low activation materials in plasma environment.

#### **Summary**

Within world fusion science research, the DIII-D National Program aims to retain leadership in advanced tokamak research and in high temperature plasma science. In so doing, results from DIII-D research will be of benefit to other magnetic confinement configurations and will serve as a test bed for several enabling and innovative technologies.



## 1.4. THE DIII-D PROGRAM INTERNATIONAL ROLE

DIII-D advanced tokamak research is carried out with extensive international collaboration to provide opportunities for scientific confirmation and joint experiments. Worldwide tokamaks (with characteristics listed in Table 1) have research programs which differ and complement each other; a summary of research capabilities is given in Table 2. International databases enable documenting accomplishments, comparing results of experiments and theory, and coordinating research. U.S. tokamaks make vital contributions to the world program with a focus on concept innovation and optimization.

**Table 1**  
**Characteristics of Operating World Tokamaks**

	Plasma Current (MA)	Magnetic Field B(T)	Major Radius R (m)	Comment
Performance Extension Tokamaks				
JET	6.0	4.0	3.0	E.U.
JT-60U	3.0	4.4	3.3	Japan
DIII-D	3.0	2.1	1.7	U.S.
Alcator C-Mod	2.0	9.0	0.65	U.S.
Tore Supra	1.7	4.0	2.3	France (superconducting)
ASDEX Upgrade	1.6	3.1	1.7	Germany
Proof-of-Principle Tokamaks				
FT-U	1.6	8.0	0.93	Italy
TCV	1.2	1.4	0.88	Switzerland
TEXTOR	1.0	3.0	1.75	Germany
JFT-2M	0.5	2.2	1.3	Japan
T-10	0.4	3.0	1.5	Russia
Compass-D	0.4	2.1	0.55	England
Triam-1M	0.15	8.0	0.84	Japan (superconducting)
Concept Exploration Tokamaks (partial list)				
JFT-2M	0.5	2.2	1.3	Japan
ET	0.3	0.25	5.0	U.S./UCLA
Truman-3M	0.18	1.2	0.5	Russia
HBT-EP	0.025	0.35	0.95	U.S./Columbia U.
Steady State Tokamaks (under construction)				
KSTAR	2.0	3.5	1.8	Korea (2004)
HT-7U	1.0	3.5	1.7	China (2004)
SST-1	0.22	3.0	1.1	India (2002)

**Table 2**  
**World Advanced Tokamak Research Capabilities**

Research Facility	Unique Research Capability
<b>Performance Extension Tokamaks</b>	
JET (E.U.)	DT capability at large size
JT-60U (Japan)	Long pulse high performance physics at large size
DIII-D (GA)	High shape flexibility, high beta, divertor, ECH
Alcator C-Mod (MIT)	High field, high density divertor
Tore Supra (France)	Long pulse superconducting
ASDEX Upgrade (Germany)	AT physics
<b>Proof-of-Principle Tokamaks</b>	
FT-U (Italy)	High field, IBW
TCV (Switzerland)	High elongation
<b>Concept Exploration Tokamaks</b>	
ET (UCLA)	High beta via omnigenity
HBT-EP (Columbia U.)	High beta via feedback

Comparing results from DIII-D with the two larger higher-temperature European and Japanese devices provides an opportunity to extend DIII-D research results and understanding to a larger scale. The European JET can operate with D-T plasmas, while the Japanese JT-60U research focuses on steady-state high-performance plasmas. Three mid-size divertor tokamaks are equipped with sufficient plasma heating, control, and diagnostic systems to carry out advanced tokamak research on a broad front. DIII-D is a low-field tokamak with high power heating including ECH for high-beta advanced tokamak research. DIII-D is unique worldwide with its poloidal field magnet capability for extensive research in plasma shaping and to emulate other tokamak shapes for coordinated joint research. Alcator C-Mod is the world's highest-field tokamak, capable of very high-density operation with equal electron and ion temperatures, with plasma pressure equal to that expected in a reactor. Its compact size and closed divertor configuration offer unique capabilities for studying high power-density plasma exhaust physics. Together DIII-D and Alcator C-Mod provide data from two plasmas with very different physical parameters but similar dimensionless parameters. The German ASDEX-Upgrade has external plasma shaping control coils of more reactor relevance but with less shape flexibility than DIII-D. Three non-divertor tokamaks, TEXTOR, FTU, and Tore Supra address pumped limiter, high field physics and steady-state current drive, and heat removal respectively. Korea is constructing a superconducting advanced tokamak (KSTAR), and China is engineering the design of a superconducting tokamak (HT-7U). DIII-D collaborates with all these international tokamaks.

Two U.S. experiments contribute to tokamak concept exploration. The Columbia University high beta tokamak (HBT-EP) is addressing wall stabilization and active mode control, issues critical for advanced tokamak operation now being extended to DIII-D. The UCLA Electric Tokamak (ET) is a low-curvature electric tokamak built to explore the possibility of achieving classical confinement and unity beta in tokamaks.

The National Academy has suggested research program strengths can be classified as to their leadership uniqueness in the context of related world programs. In this respect, DIII-D is unique in its plasma shape flexibility, its high beta research including feedback stabilization, its comprehensive transport diagnostics, its ECCD profile control capability, and its advanced tokamak divertor program. DIII-D pioneered advanced tokamak concepts through an integrated approach to fusion energy science and is a leading supplier of results to international physics databases. DIII-D is among world leaders in ICRF (having pioneered fast wave current drive), in the study of neoclassical tearing modes (collaborating with AUG and JET), and in pellet fueling. DIII-D does not commit significant resources to a number of research areas where others have strong leads. These areas include large scale facility size, D-T capability, LHCD, and metallic divertor. From the above classification it is evident that DIII-D strives for leadership in several areas of fusion science and physics innovation rather than in fusion technology where other world facilities lead.

## 1.5. RESEARCH PLAN LOGIC

Our long range AT Program will evolve in two phases. First to establish the credibility of the AT approach, we have set out on a three year (1999–2001) focus on demonstrating intermediate AT scenarios for 5 seconds. Two intermediate scenarios, are described in Sections 2.2.1 and 2.2.2 and will be carried out with lower toroidal field, plasma current, and EC power less than our ultimate objective. Achievement of this intermediate objective in 2001 will provide a basis point for pressing on to the second phase of our AT program, developing deeper scientific understanding of AT physics, and exploring the ultimate potential of the tokamak. That potential, as defined by theory calculations of stability and the residual transport after ITG turbulence is suppressed involves very broad pressure profiles, transport barriers near the plasma edge, nearly 100% bootstrap current in a peak near the edge, and very high normalized beta supported by effective wall stabilization systems. These more challenging investigations as well as our intermediate scenarios will be extended to 10 second pulses at full (2.1 T) toroidal field in DIII-D. These ultimate scenarios are described in Section 2.2.3.

The logic diagram for the DIII-D Advanced Tokamak Program has been revised to take account of progress in 1999 and is shown in Fig. 1. The main line is the pursuit of

## THE 2000 DIII-D ADVANCED TOKAMAK RESEARCH THRUSTS FOR 2000–2004

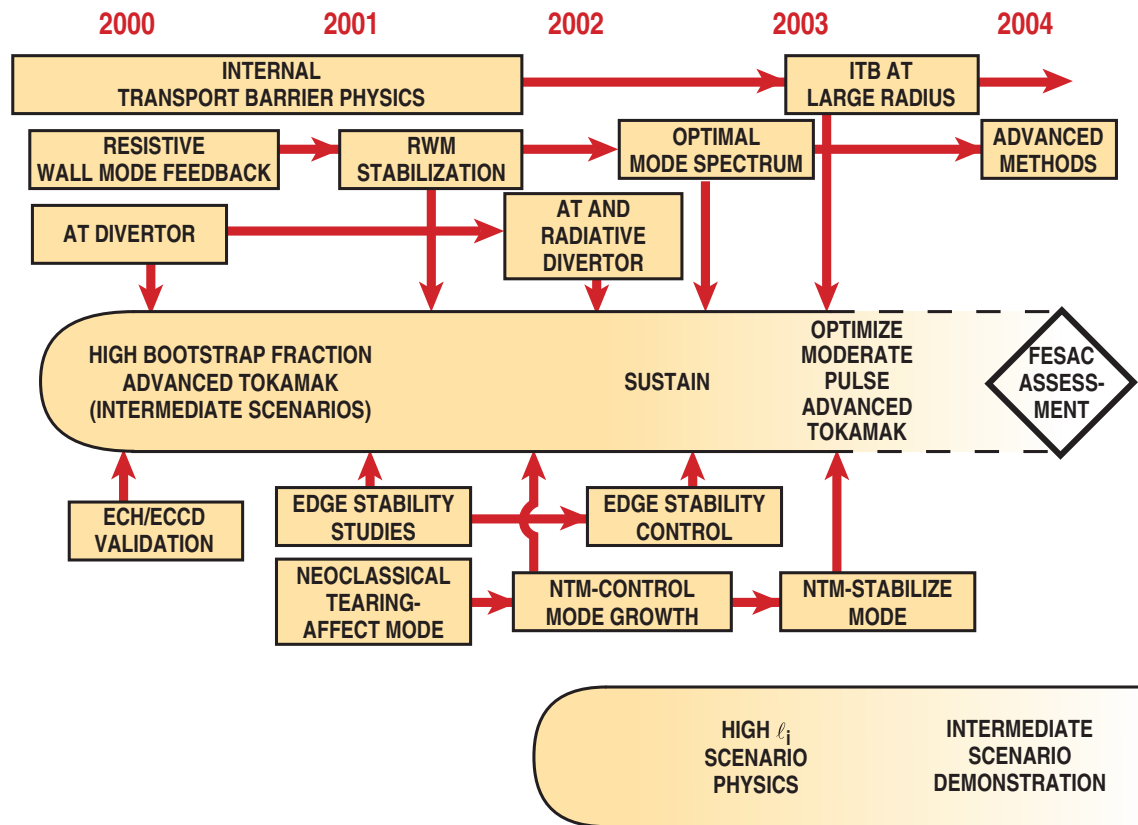


Fig. 1. Logic diagram for the DIII-D Advanced Tokamak Program.

the high bootstrap fraction AT scenario. This scenario was described as the negative central shear scenario in Section 2 because it derived from the exciting negative or reversed shear discoveries in tokamaks in the last few years. However, since our results to date have been most positive with weak or slightly positive shear, we have called this line of AT research simply the high bootstrap fraction scenario in this diagram and in our research thrust lists. The matter of whether the optimal shear is negative or weakly positive will be decided by the research. Good progress was made on this scenario in 1999. To prepare for the new but limited ECCD power in 2000, this scenario begins at the reduced current and field of 1.2 MA and 1.6 T. In 1999, without any active current profile control, discharges with  $\beta_N H_{89} \sim 9$  for 2 seconds (16 energy confinement times) were achieved, exceeding our expectations for 1999 preparatory work. The duration of these discharges was limited by the uncontrolled inward diffusion of the current profile which resulted in the growth of a resistive wall mode. Hence the next order of business in this research line is to apply ECCD power in 2000 to counteract the resistive diffusion of the current. Success in that endeavor will set the basis for longer pulse sustainment of these discharges, but owing to the limited pulse length of the gyrotron set in 2000, the actual longer pulse sustainment will be sought in 2001 and 2002 when most of the EC

power is available from the long pulse tubes. As more ECCD power becomes available throughout 2000–2002, we will increase the field and the current at which this scenario is developed with the intent of reaching 1.6 MA current at full field (2.1 T) in DIII-D in 2002. Further increases in long pulse EC power and the magnet pulse length will culminate in DIII-D being the laboratory for the study of the moderate pulse advanced tokamak called for in the FESAC goals.

Two research thrusts in 2000 should be of one year duration and are in direct support of our AT scenario thrust. The thrust on ECH/ECCD validation provides specific runtime to bring into physics operation the new gyrotron systems. Our commitment is to have four gyrotron physics operation in 2000; we have six gyrotrons in-house and are working to get at least five operational. Work in this thrust will demonstrate that local heating and current drive can be obtained from these gyrotrons and some physics experiments using them will be carried out under this thrust. This thrust should be of one year duration with the EC physics studies reverting to the Heating and Current Drive Topical Area in 2001 and thereafter.

The AT divertor thrust will bring into operation the now highly baffled and fully pumped upper divertor that enables increased pumping of the high triangularity plasmas to be studied in the AT scenario work. This thrust will develop the basic understanding of particle control preparatory for the AT scenario, including a first look at impurity control by means of strong fuel ion flows in the scrape-off layer. Further research using this divertor will probably be carried out in the Edge and Divertor Physics Topical Area in 2001. In 2002, we anticipate a strong effort to explore coupling the AT scenario with a radiative divertor, work essential to eventual integration of the core and divertor physics efforts.

In the pursuit of this scenario in 1999, results learned about the instabilities which can terminate AT modes have affected the choice of research thrusts in 2000. Since the mode this primary scenario has encountered as limiting is the resistive wall mode, the research thrust on the resistive wall mode will continue in 2000. The necessary feedback amplifiers for the present six coil system were made operational a year ahead of schedule in 1999 to get a first look at feedback interaction with the RWM. However much work remains to be done on the basics of the physics and the feedback methodologies and so the RWM work will proceed in parallel with the AT scenario work. Application of the RWM system to stabilization of the RWM is anticipated in 2001. A substantial increase in the stable normalized beta is predicted if the present six coil RWM system is expanded to 18 coils to optimize the mode spectrum. Research using this optimized 18-coil system will begin in 2002. More advanced wall stabilization approaches using systems internal to the DIII-D vacuum vessel may be studied later.

Our AT scenario in 1999 surprisingly went smoothly into an ELMing H-mode edge without encountering the terminations of high performance from edge instabilities prominent in most previous AT efforts on DIII-D. We have developed a detailed understanding of the edge instabilities involving second stable ballooning access afforded by the edge bootstrap current. In 1999, our research thrust on edge instabilities made progress on developing methods to actively intervene in the edge stability situation. However, since our primary scenario was not limited by edge instabilities in 1999 and since runtime is very limited, we have not allocated specific runtime to the Edge Stability Thrust in 2000. Another factor in this decision was that we are developing a lithium beam based diagnostic to measure the edge current density and the availability of that diagnostic will illuminate the further study of the edge instabilities in 2001 and 2002. This course runs the risk that our primary AT scenario will reencounter the edge instabilities as the field and current are raised. A preliminary search for such future problems may be made in the AT scenario thrust in 2000. Some work also continues on the Edge Stability in the Stability Topical Area in 2000.

Our AT scenario in 1999 was also not limited by neoclassical tearing modes. Hence we have also have not allocated specific runtime to the Neoclassical Tearing Mode Thrust in 2000. This decision was somewhat difficult since the ECCD power will be available in 2000 to begin the very interesting research in stabilizing NTMs with local ECCD. Some work on this research line using the ECCD has been planned in the Stability Topical Area in 2000. We anticipate returning to a focus on this NTM work in 2001 with an emphasis on studying how to use ECCD to affect the modes, followed by work in 2002 on shrinking the magnetic islands and work in 2002 on stabilizing the NTM. If our AT scenario reencounters the NTM limitation, we may have to accelerate the work on NTMs and can do so.

Our research thrust on Internal Transport Barriers is aimed at longer term optimization of AT scenarios. Theory work has pointed to ultimately very advanced states of tokamak performance with nearly 100% bootstrap current in a very hollow profile with a peak near the outer edge of the plasma produced by a broad pressure profile with a transport barrier near the plasma edge. In the long run, it will be desirable to move the transport barrier location to a large radius. Very exciting exploratory work on ITBs was done in 1999 using counter injection to alter the radial electric field profile to affect the  $E \times B$  turbulence shearing rate with the result of moving the radius of the foot of the transport barrier from  $\rho \sim 0.4$  using co-injection to 0.6 using counter injection. Favorable results were also obtained using neon to lower turbulence growth rates. Exploratory results on using inside-launch pellet injection to form transport barriers were also obtained. This work is important to the long term since relatively more bootstrap current can be obtained from a density gradient than from a temperature gradient, within an overall stability constraint on the pressure gradient. This important work for the long term

will continue (albeit at a reduced level) in 2000 with an eventual goal (~2002) of contributing the knowledge base to further optimize the AT scenarios we will have developed by that time.

Another longer term AT research objective is to open a second major line of AT work, the High  $\ell_i$  Thrust, starting in 2002. Limited runtime forced a choice between the NCS and High  $\ell_i$  AT lines in 1999. We have placed our primary effort on the NCS or high bootstrap fraction line in the near term. But the high  $\ell_i$  scenario is also a credible path to an Advanced Tokamak future. We intend to restart work on this scenario in 2002 with the initial physics investigations of active stabilization of the sawtooth instability by fast waves followed by the development of scenarios using fast wave, electron cyclotron, and neutral beam heating and current drive power in later years. This next major research line can be expected to develop a logic diagram as complex as that shown in Fig. 1 for the high bootstrap fraction scenario.

### **Facility Capabilities**

The Advanced Tokamak facility capabilities needed to accomplish this research are shown in Fig. 2. The key hardware capability being implemented is high power, long pulse gyrotrons. The new gyrotrons are nominal 1 MW output power and are equipped with diamond windows for 10 second operation in DIII-D. Experiments in the year 2000 will be conducted with four gyrotrons. Two gyrotrons have the new diamond windows. One is an old developmental prototype and the other is the first production tube of the new diode gun design. The other two gyrotrons will be older units limited to 2 second pulses. This complement of EC sources will enable us to attempt the high bootstrap fraction scenario identified as four tubes (2000) in Table 3. Two additional new production tubes will become available in the year 2001, so we can then begin experiments attempting the high bootstrap fraction scenario at the higher parameters identified as six tubes (2001) in Table 3. To enable the AT studies at longer pulses and full field and beyond our intermediate scenarios, two more production unit gyrotrons will become available in 2002. In 2003, the EC system power will be brought to the full power called for in the scenarios described in Section 2.2.3 by the installation of three higher power (1.5 MW) gyrotrons being developed by the Virtual Laboratory for Technology.

For density control, the upper divertor private flux baffle and inner leg pump which were installed at the end of 1999 are expected to give us the required density control for high triangularity plasmas using the upper pumps or for low triangularity plasmas using the lower pump. Because of the importance of triangularity, the upper divertor density control capability is an essential element of the AT scenario thrust in the 2000 campaign.

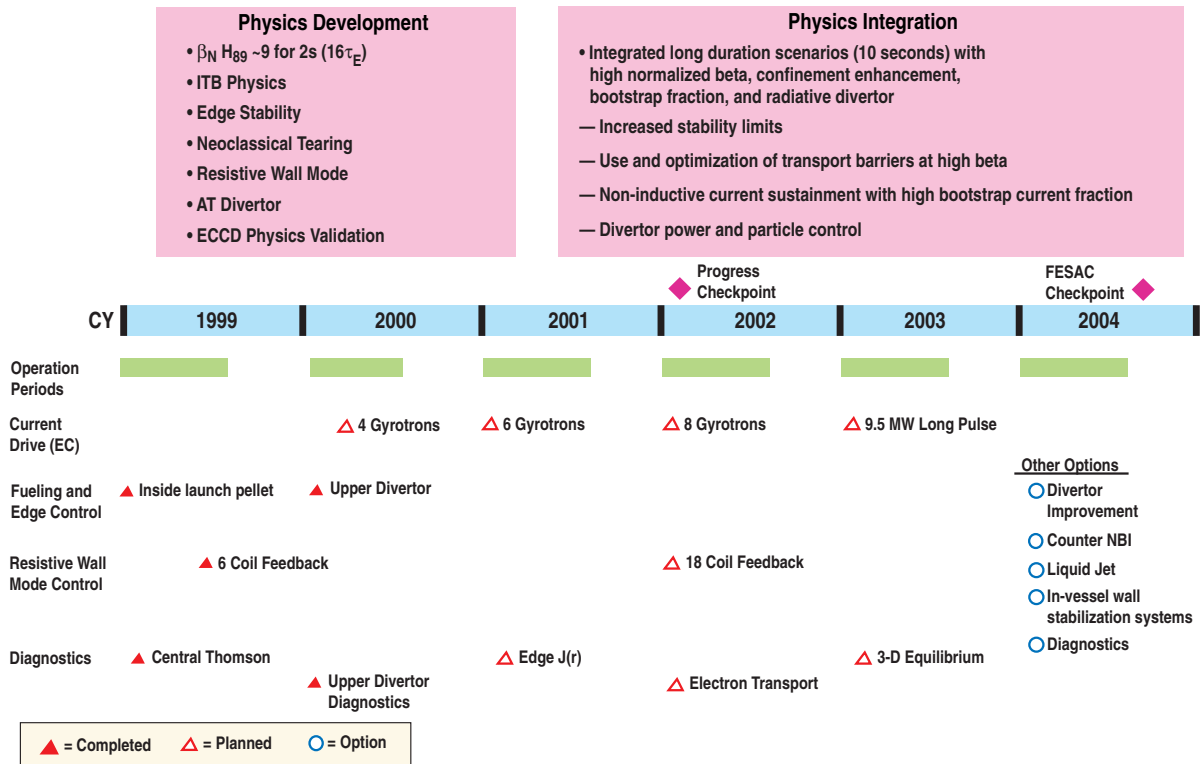


Fig. 2. DIII-D Advanced Tokamak Five-Year Research Plan.

The new upper divertor will also allow resumption of the studies of optimizing the core/divertor plasma performance balance by better retaining neutrals and impurities in the divertor using copious flows in the scrape-off layer (puff-n-pump in DIII-D jargon). This effort to make a divertor compatible with an AT core may be also applied to the NCS scenario effort in 2001.

The pellet fueling capability, extended to inside launch in 1999, proved valuable in triggering internal transport barriers in the density channel. This pellet fueling capability will be further utilized to explore transport barriers and to extend the AT thrust beyond the intermediate scenarios (post 2001).

The wall stabilization work made a good beginning in 1999 with initial development of feedback control using a six-coil system and by accelerating three power supplies originally planned for 2000. Studies in 2000 and 2001 will focus on the basic physics of wall stabilization and on validation of quantitative models for feedback stabilization. Modeling results indicate that such an extension of the system to 18 coils could significantly increase the margin over the no-wall stability limit which can be achieved with feedback stabilization. Two new toroidal arrays of 12 saddle loops each, above and below the midplane, will be available in 2000 to improve our measurements of resistive wall



mode structure. These loops are also expected to serve as the sensors for the 18-coil system. The 18-coil resistive wall mode (RWM) feedback system is planned for the 2002 campaign to optimize the normalized beta that can be held by wall stabilization in DIII-D.

Enhanced diagnostic capabilities will support the evolving AT research plan. A lithium beam diagnostic will be added for the 2001 campaign to enable measurement of the edge current density profile to significantly enhance the scientific understanding of edge MHD instabilities related to the edge bootstrap current, which we believe opens second regime access. This increased understanding will be important in developing techniques for preventing edge MHD instabilities from terminating high performance AT phases. Although important work remains to clearly identify ITG modes in a plasma, the transport frontier is moving on to the yet smaller wavelength turbulence probably responsible for the residual anomalous electron transport when the longer wavelength turbulence has been suppressed by sheared  $E \times B$  flows. An initiative in diagnostics for this electron transport is planned. After the complete installation of the resistive wall mode feedback system is completed, a set of diagnostics to enable reconstruction of 3-D, non-axisymmetric equilibria is planned.

Over the three year period 2001–2003, as physics progress pushes out to longer duration AT phases, a set of modest modifications to the thermal capacity of the DIII-D toroidal coil connections and poloidal coil power supplies will be made to bring the pulse length to 10 seconds. The radiative divertor physics will be called upon then to provide sufficient radiative heat dispersal in the divertor to enable 10 second pulses and thereby, to fully integrate AT operation with effective divertor operation.

## 2. ADVANCED TOKAMAK PROGRAM PHYSICS

### 2.1. PHYSICS ELEMENTS OF THE PRINCIPAL AT SCENARIOS

The goal of the DIII-D program is to establish the scientific basis for the optimization of the tokamak approach to fusion energy production. This scientific research has many elements, but the principal focus of the DIII-D program toward achieving this optimization is the advanced tokamak program. The advanced tokamak program is aimed at improvement of the tokamak concept towards higher performance and steady-state operation through internal profile modification and control, plasma shape, and MHD stabilization. The dependence of the core performance on the boundary conditions, and the operational regimes envisioned, put more stringent requirements on the divertor and edge plasma, leading to inclusion of divertor optimization and control in any tokamak optimization program.

Two characteristics make the optimization of tokamak performance “advanced”: the inherent one and two dimensional dependence of tokamak performance on the plasma profiles, shape, and boundary; and the requirement to develop solutions that are both multidimensional and self-consistent. The performance capabilities and limitations of the tokamak, and requirements for an energy producing tokamak have long been communicated in terms of global zero-dimensional parameters and largely empirical scaling relations. Chief among these scaling relations are the confinement scaling relations and the scaling of beta with normalized current, known as Troyon scaling. More recently we have discovered, both experimentally and theoretically, that the performance of the tokamak plasma also depends largely on the details of internal plasma profiles, details of the plasma shape, and details of the plasma boundary.

This improvement in our understanding depended critically on the development of new diagnostics to measure the important profile parameters, such as the motional Stark effect diagnostic for measuring the internal magnetic field structure, the charge exchange recombination system to measure toroidal and poloidal plasma flows, and many new turbulence measurements. These new measurements lead to discovery and appreciation of new and important physics phenomena in the tokamak, such as the role of sheared  $\mathbf{E} \times \mathbf{B}$  flow, and neoclassical tearing modes.

Equally important to new diagnostic capability is the development of new theories and modeling capabilities to put the transport, stability, and current drive projections on a firmer physics basis. An excellent example of the modeling and theory progress is in

gyro-kinetic and gyro-fluid approaches for physics based transport calculations, and the appreciation of the importance of sheared  $\mathbf{E} \times \mathbf{B}$  flow in the predictions.

The self-consistency of the parameters and profiles of high performance plasmas is one of the leading challenges of the advanced tokamak program. As well as the details of both the current density and pressure profile impacting the ideal stability limit and stability to non-ideal modes, at high beta the self-generated bootstrap current is necessarily a major component of the total current. Since the profile of the bootstrap depends on not only the profile of the pressure but of its individual constituents (density, electron temperature, ion temperature, ...), the pressure profile and the current density profile are not separable. But, the pressure profile is determined by the transport profiles. In turn, the details of the pressure profile and the current density impact the turbulence growth rates and sheared  $\mathbf{E} \times \mathbf{B}$  flow which predominantly determine the transport. In a final advanced tokamak scenario, these interdependencies and complex non-linear relationships must be fully taken into account and fully integrated. This process greatly benefits from and contributes to the development of a strong fundamental (first principal) physics basis for fusion science.

The DIII-D Advanced Tokamak program aims to develop the best possible operational scenario for fusion energy production using the tokamak. There are many opportunities to make improvements, and many complex interdependencies that allow for a multitude of possible advanced tokamak solutions. In this context it is important to recognize that our rapidly developing understanding and new innovations can lead to scenarios that we do not now envision. So, in developing the “scientific basis for optimization of the tokamak” we consider of paramount importance to maintain an attitude of research that is open to new discoveries and continual improvements. We therefore try to plan a DIII-D program that is not only targeted toward testing specific scenarios, but is also optimally positioned to take advantage of new discoveries and innovations. This translates directly into developing diagnostic and control capabilities that are flexible and versatile.

To make significant progress in our research, it is important nevertheless to focus on testing specific scenarios while being alert for discovery. It is important to set aggressive and measurable goals (targets) toward which to focus our efforts. We take our best present understanding of the physics and our best vision of the future embodiment in an energy producing system and develop scenarios, which we can test experimentally in the DIII-D device.

Consideration of physics and energy production lead us naturally to two principal steady-state advanced tokamak scenarios. These two scenarios are negative central magnetic shear (NCS) and high internal inductance (high  $\ell_i$ ). These two scenarios do not

encompass all the known approaches to tokamak improvement, but rather provide some focus to the challenges that confront us. The profiles and conditions of the two scenarios are quite different, but it is recognized that a fully optimized scenario might lie somewhere in the space between the two.

The viability of a tokamak as an economically and environmentally attractive power plant requires both sufficient energy confinement time,  $\tau_E$ , for ignition margin, and sufficient volume average toroidal beta,  $\beta_T = 2\mu_0 \langle p \rangle / B_T^2$ , for adequate fusion power density. Further improvements in the tokamak reactor concept can be made if these improvements in  $\beta_T^{\max}$  and  $\tau_E$  are obtained in steady-state discharge conditions (Kikuchi 1993). We are seeking scenarios that have the potential for high beta, high confinement consistent with steady state, and consistent with divertor scenarios that can provide adequate heat removal, particle and helium ash control, and impurity control.

A minimum necessary condition for an attractive fusion energy producing system is high energy gain. Some insight into possible operational scenarios is obtained by considering the energy gain for a steady state system, given by Eq. (1):

$$Q \propto \frac{P_{\text{fus}}}{P_{\text{CD}}} = \frac{P_{\text{fus}}}{\frac{n R I_P}{\gamma_{\text{cur}} (1 - f_{BS})}} \propto \frac{\gamma_{\text{cur}} \epsilon_{\text{eff}} \beta_N^2}{n q (1 - \xi \sqrt{A q} \beta_N)} \quad (1)$$

In Eq. (1),  $P_{\text{FUS}}$  is the fusion power, the  $P_{\text{CD}}$  is the current drive power,  $\gamma_{\text{CUR}}$  is the current drive efficiency,  $\epsilon_{\text{EFF}}$  is the effective inverse aspect ratio,  $A$  is the aspect ratio,  $q$  is the safety factor at the plasma edge,  $\beta_N$  is the normalized beta and  $f_{BS}$  is the fraction of the total current that is the self-driven bootstrap current. In any steady state scenario, care must be taken to minimize the current drive power required. One can view two separate approaches (NCS or high- $\ell_i$ ) to minimizing this current drive power: (1) maximize the bootstrap fraction, or (2) maximize the efficiency of current drive ( $\gamma_{\text{CUR}}/nI$ ). If the bootstrap fraction becomes a major fraction of the total current, the current profile becomes naturally hollow with the maximum off-axis and the central portion of the plasma has negative central shear, NCS. The bootstrap fraction is further increased by increasing the minimum value of  $q$ ,  $q_{\min}$ , and moving the radius of the  $q_{\min}$  to larger radius. If the emphasis is placed on increasing the current drive efficiency, it is natural to drive the current on axis where the temperature is highest (current drive efficiency is proportional to electron temperature) and where the effects of trapping are minimal. Axial current drive leads naturally to peaked current densities, with large positive magnetic shear in the outer plasma region. A schematic of the resultant current profiles is shown in Fig. 3. The actual current profile for these two cases depends on establishing consistency among the profiles, stability, and transport.

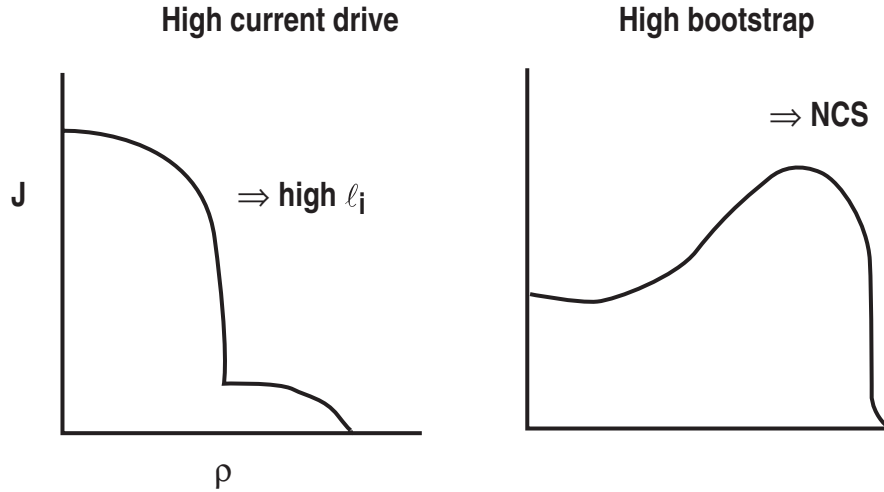


Fig. 3. Steady state considerations also lead to two “natural” current profiles.

Unless the NCS scenario has fully 100% bootstrap driven current, it is important to maintain relative high current drive efficiency in both the NCS and high  $\ell_i$  scenarios.

The need for high current drive efficiency pushes steady state operational regimes to higher temperature and lower density than might otherwise be the optimal in a Ohmically pulsed scenario. The higher temperature and lower density, impose new challenges for heat removal and impurity control for the divertor. This lower density, higher temperature operation motivates the inclusion of divertor optimization as an important element in the DIII-D AT program.

Simple physics considerations also lead to the same operational scenarios, (1) NCS and (2) high  $\ell_i$ . We show in Fig. 4, the general dependence of ideal ballooning stability and ion temperature gradient (ITG) driven instabilities on the magnetic shear,  $S_M = \rho/q (\partial q/\partial \rho)$ . These general dependencies, known for a long time, clearly show that both low or negative magnetic shear and high magnetic shear are favorable for stability of ballooning modes and ITG modes. These physics considerations lead to the same two general classes of scenarios given above; (1) low or negative shear  $\rightarrow$  NCS, and (2) high positive shear  $\rightarrow$  high  $\ell_i$ . It is worth noting that the magnetic shear (in the large aspect ratio circular limit) observed experimentally in Ohmically driven discharges is near 1, nearly the most unfavorable value for ballooning and ITG mode stability. So one might expect that the ability to modify the current profile toward either larger positive or negative magnetic shear would lead to positive benefits.

### 2.1.1. General NCS Considerations

The NCS scenario has the potential for a high bootstrap fraction at moderate  $q$ : the bootstrap fraction can approach unity at  $q_{95} = 5-6$ . Furthermore, there is the potential for the bootstrap current to be well aligned with the total current, resulting in low, total current drive requirements. The hollow current profile, and the resultant region of negative central magnetic shear derive naturally from the bootstrap current. The bootstrap current is proportional to the square-root of the local aspect ratio times the pressure gradient, both of which go to zero on axis, so that the bootstrap current profile is naturally hollow. In addition, the higher axial  $q$  and lower poloidal field in the core have the effect of increasing the total bootstrap fraction. The high bootstrap fraction results in lower total current drive, but highly localized, off-axis, precision current drive is needed. Electron cyclotron current drive is well suited for the precise off-axis current drive needed. Because of the potential of the NCS scenario with respect to fusion energy, we have chosen it as the leading scenario on which to focus.

The NCS scenario does have some very specific challenges. The first challenge is stability. Stability to ballooning modes is a necessary condition for achieving high beta, and therefore an important consideration. The NCS scenario avoids ballooning mode limitations because the region of high pressure gradient is in the region of low or negative shear, where there is access to the second regime and no limiting pressure gradient is calculated. Furthermore, the negative shear region is stabilizing to neoclassical tearing modes where the pressure gradient is expected to be large, and if the minimum value of  $q$  is above 2, the absence of low order rational surfaces should further diminish the importance of the modes.

There are several MHD instabilities that remain a challenge to the NCS scenario. Strong pressure gradients in the region of negative shear can be destabilizing to resistive

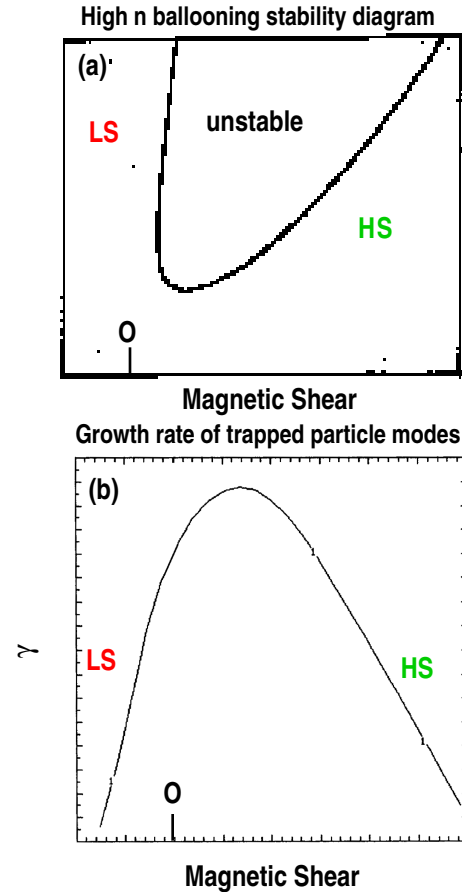


Fig. 4. Both low magnetic shear (LS) and high shear (HS) are favorable for: (a) higher beta, (b) reduced turbulence and reduced transport. Magnetic shear is  $s \propto R/B_T q^2 dp/dr$ .

interchange modes. Modeling indicates that these modes are stable if the magnitude of the negative shear is kept modest. Double tearing modes are calculated to be unstable as a consequence of the double value of  $q$ . However, these are rarely observed in the experiment, and modeling indicates modest rotational difference in the plasma between the two surfaces (as observed in the experiment) is sufficient for stabilization.

The NCS scenarios have quite low  $\ell_i$  and are generally unstable to the external/global kink, in the absence of a conducting wall. However, the broad current density profile, broad pressure profile, and strongly shaped plasmas couple very strongly to a nearby wall. Modeling indicates that  $\beta_N > 5$  stable to  $n=1$  and 2, is easily obtained if a conducting wall is located at  $r_w/a < \sim 1.5$ . The modeling calculations for  $n=1$  are shown in Fig. 5. However, the real wall is resistive and the plasma is subject to the resistive wall mode. The stabilization of the resistive wall mode then is key part of validating and optimizing the NCS scenario. The DIII-D program is taking two approaches to stabilization of the resistive wall mode; passive stabilization with a rotating plasma in the presence of a resistive wall, and active feedback stabilization with non-axisymmetric external coils.

It is important to note that reasonably high beta values can be calculated for the NCS scenario without a conducting wall;  $\beta_N$  values  $< 4$  are calculated, very similar to the high  $\ell_i$  scenario. So if wall stabilization proves not to be so attractive in a reactor embodiment, there remain attractive NCS and high  $\ell_i$  scenarios.

For the NCS scenario, perhaps the most challenging physics lies in the consistency of the profiles. A range of current density and pressure profiles can be identified that are consistent with high beta stability. In particular, it can be shown that broad pressure profiles are required for high beta stability and alignment of the bootstrap current (Fig. 6). However, the combination of the  $q$  profiles, pressure profiles, and rotation ( $E \times B$ ) profiles often result in transport reduction and often the formation of a clear internal transport barrier that leads to pressure peaking that are not compatible with high beta.

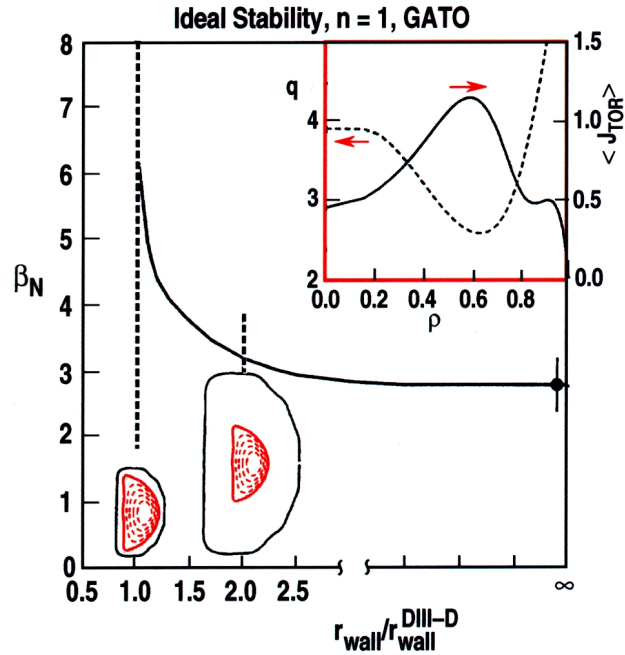


Fig. 5. Maximum stable beta increases for closer wall position: ideal  $n=1$  stability using DIII-D plasma shape and DIII-D wall. Insets are typical current density and  $q$  profile (Taylor1995).

Discharges in DIII-D can have an internal transport barrier, ITB, with no edge transport barrier (L-mode NCS), a strong edge transport barrier, (H-mode NCS), and a self-regulating edge barrier with an internal transport barrier (ELMing H-mode NCS). These three cases have different challenges with respect to high beta and self-consistent solutions. The L-mode NCS has a very weak pressure gradient in the outer portion of the plasma. The key challenge for L-mode NCS is to move the transport barrier to larger major radius to achieve higher beta [as shown in Fig. 6(a)] and to obtain good bootstrap alignment. It is also important that for stability, the width of the transport barrier region not become too narrow as indicated in Fig. 6(b). In general, peaked pressure profiles that result from an ITB at small radius result in a low stability limit as shown in Fig. 7. The ELMing H-mode NCS and the H-mode NCS both lead to broader pressure profiles and the potential for high beta with an ITB. For the ELMing case, the repetitive ELMs provide a seed for neoclassical tearing modes, and the higher pressure gradient in the positive shear region make the neoclassical tearing modes unstable. For H-mode NCS, a clear strong barrier exists near the boundary, and the plasma is subject to low  $n$  kinks associated with the high edge pressure gradient and high edge current density. High beta, broad profiles, and strong shaping cause strong harmonic coupling and these edge driven modes are no longer localized to the edge. The key challenge for the H-mode NCS scenario is to understand how to moderate the edge and avoid the edge instability or its strong coupling to the core.

A physics understanding of the edge instability is unfolding and we are developing techniques to modify and control these instabilities. In DIII-D the edge pressure gradient is limited by moderate  $n$  ( $2 \lesssim n \lesssim 9$ ) kink/ballooning instabilities. These modes are driven

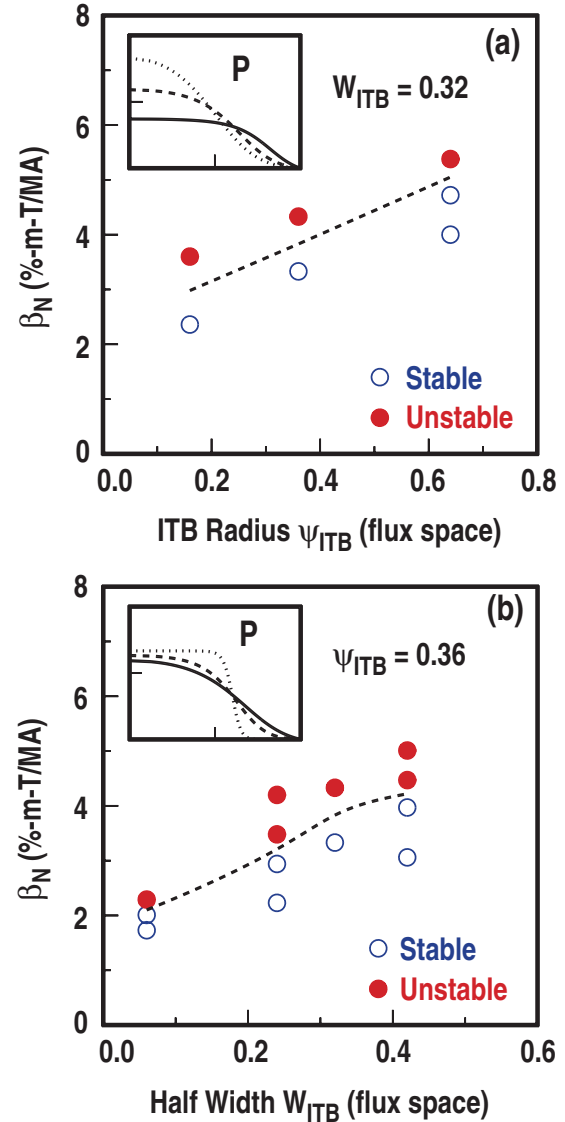


Fig. 6. Stability limit improves with internal transport barrier width and radius. Fixed shape DND,  $q_{95} = 5.1$ ,  $q_0 = 3.2$ ,  $q_{min} = 2.2$ ; hyperbolic tangent pressure representation; ideal  $n = 1$ , wall at  $1.5a$ .



by both the locally high pressure gradient and the locally high edge current density (the edge current density is the bootstrap current driven by the edge pressure gradient). The edge region is typically in the region of second stable access to infinite  $n$  ballooning modes, and local pressure gradient is significantly higher than that expected from the first regime limit. High squareness shaping eliminates the access to second regime stability and leads to much smaller and more frequent ELMs (presumably at higher  $n$ ) more compatible with an internal transport barrier. Edge impurity radiation reduces both the edge pressure gradient and the edge current density and also gives smaller and more frequent ELMs. Both plasma shaping and edge impurity radiation are being evaluated as techniques to control the edge instabilities, and better measurement of the edge current density with Li beam polarimetry is being pursued in order to better quantify the edge stability models.

A sound physics understanding of the reduced transport in the NCS discharges, and of the transport barrier formation, is developing based on sheared  $E \times B$  flow stabilization of microturbulence. An extremely rich variety of physics effects provide for exciting and interesting fusion science research, as well as opportunities for control of the transport and transport barrier. The ability to vary the location of the internal transport barrier and to control the magnitude of the local pressure gradient can allow us to generate pressure profiles consistent with high beta stability and bootstrap alignment; see Fig. 6.

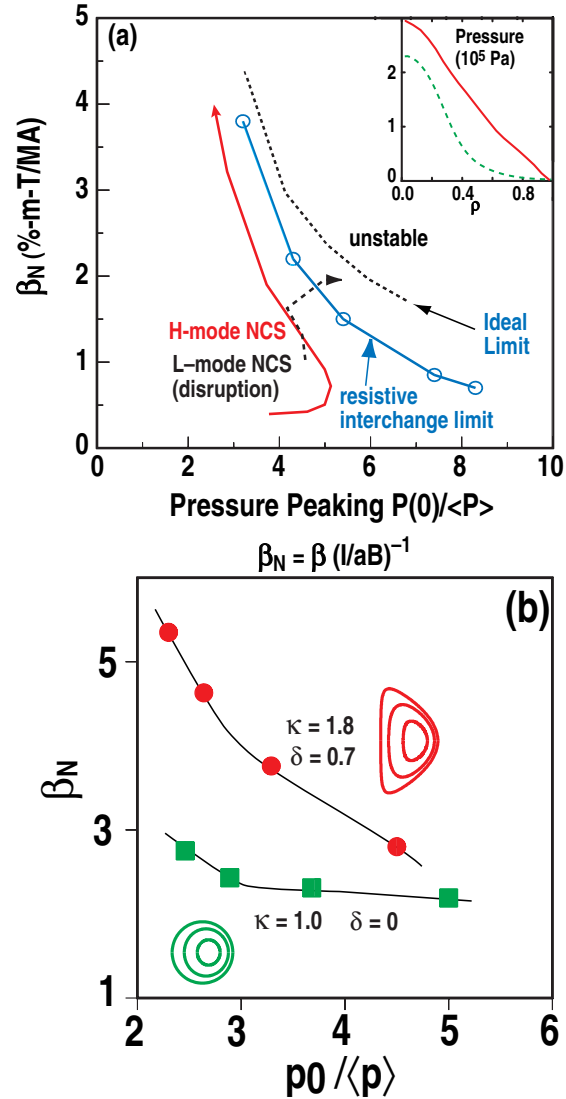


Fig. 7. Higher  $\beta$  is obtained with broad pressure profile (a) normalized beta vs. pressure peaking. Ideal and resistive limits are from generated equilibria similar to the experimental. Dashed trajectory is for an L-mode NCS discharge, solid trajectory is for H-mode NCS discharge (Lao 1996). Insets are exp. pressure profile just prior to disruption. (b)  $\beta_N$  vs. pressure peaking for D shaped and circular shaped equilibria,  $q_0 = 3.9$ ,  $q_{min} = 2.1$ ,  $q_{95} = 5.1$ ,  $rw/a = 1.5$  (Turnbull 1996).

### 2.1.2. General High- $\ell_i$ Considerations

A significant experimental basis for a high  $\ell_i$  high performance scenario exists. A number of tokamaks have observed experimentally that the maximum achievable beta increases with internal inductance, and the DIII-D experimental program has established the scaling relation  $\beta_{\max} = 4 \ell_i * I/aB$ . (Taylor 90 IAEA). This relation has been supported by a large number of experimental results from other tokamaks. It has also been shown to be consistent with theory and modeling results (Lao 1991), at least for a class of equilibria generally consistent with Ohmically driven current profiles. It has also been shown in a wide range of experiments that the energy confinement time increases with  $\ell_i$ . The increase in confinement has been shown to be a consequence of an increase in magnetic shear and a consequence of an increase in the  $E \times B$  flow shear. There exists a positive feedback mechanism between the two effects. These high confinement and high beta results have to date been achieved transiently by ramping down the plasma current or by expanding the plasma size.

Self-consistency of the profiles in steady state does place limitations on the high  $\ell_i$  scenario. Maintaining  $q_0$  slightly above unity and avoiding the  $m/n = 1/1$  sawtooth instability has been observed to be a necessary condition in achieving high performance in many tokamaks. We will make the most peaked current density profile possible (highest  $\ell_i$ ) consistent with ballooning stability and resulting allowable pressure profiles in the following way. The current profile will consist of the driven seed current and the bootstrap current. The driven seed current will have a top-hat form and is located in the core, with the limitation that  $q_0 > 1$ . The total current density is equal to the maximum of the local current density and the local bootstrap current. The pressure gradient is limited to remain below the ballooning limit. The resultant current density profile is shown in Fig. 8, and the internal inductance is limited to  $\ell_i \sim 1.1$ . The maximum beta stable to ideal ballooning modes in such a case is  $\beta_N < 4$  (for  $\kappa = 1.8$ ,  $\delta = 0.7$  equilibrium), and the maximum bootstrap fraction is limited to approximately 60% at  $q \sim 7$ . This scenario is an attractive advanced tokamak scenario, and we think the physics challenges are not very demanding. However, because of its bootstrap current limitations and implications on achievable steady state  $Q$ , the high  $\ell_i$  scenario is not our leading scenario.

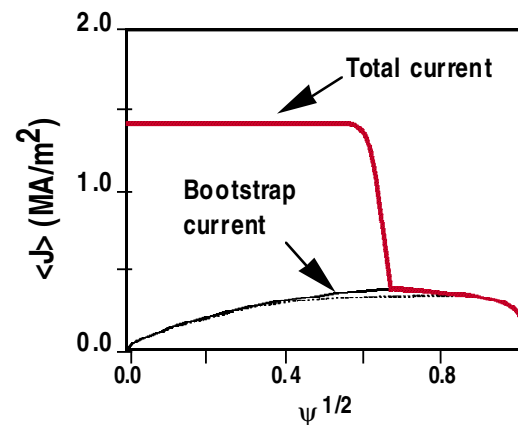


Fig. 8. Self-consistent current profile from high  $\beta$ , high  $\ell_i$  equilibrium  $\beta_N = 4$ ,  $\ell_i = 1.2$ ,  $q_{95} = 8$ ,  $q_0 = 1.05$ .

## 2.2. THE NEGATIVE CENTRAL SHEAR (NCS) SCENARIO IN DIII-D

The principal approach to the AT in DIII-D is the negative central shear regime. This regime has the best set of characteristics to take forward to a steady-state fusion reactor. The hollow current profile is compatible with the high confinement arising from a transport barrier since the off-axis bootstrap current produced by the transport barrier will produce most of the required off-axis current peak. The rest of the non-inductive current can be either on-axis for central  $q$  control or off-axis to supplement and align the bootstrap current peak with the required total current profile. The negative central shear  $q$  profile and the broad pressure profile resulting from a transport barrier and  $q_{\min}$  being at large radius are compatible with high normalized beta. Wall stabilization is also needed owing to the closer proximity of the current peak to the plasma edge. This scenario can be made with either the L-mode or H-mode edge. Which is best for stability and confinement is an active subject of ongoing research.

There is considerable flexibility in this scenario in regard to how the plasma edge is managed and how the interior current and pressure profiles are controlled. It is not clear, for example, how much magnetic shear reversal is needed, even to the limit of zero shear.

On three or four separate occasions in the last four years, different people from different viewpoints have constructed AT NCS scenarios for DIII-D using the ONETWO transport code, the stability codes GATO and BALOO, and the transport code CORSICA. We will summarize those scenarios below in order of increasing complexity of the transport modeling rather than in the chronological order in which they were done. They exhibit some different approaches and interests which provide pathways into the variations in experimental approach being currently pursued and we will comment on those pathways into the ongoing experimental program. Recent work on defining optimum scenarios for ARIES-AT also point to exciting long-term directions for the DIII-D research.

### 2.2.1. Scenarios Using Fixed Profiles

The purpose of this modeling exercise was to demonstrate the potential for intermediate advanced tokamak operation goals at intermediate values of plasma current and toroidal field with the view of a phased installation of a ten gyrotron system (nominal 1 MW/gyrotron source with 70% delivered to the plasma) for ultimate operation at full field and current in DIII-D. For this purpose scenarios with 3, 6, and 10 gyrotrons were developed from  $B_T = 1.6$  T to full  $B_T = 2$  T and  $I_p$  ranging from 1.0 MA to 1.6 MA.

The starting point in each case was a stable MHD equilibrium with boundary consistent with the full RDP installation. Only the total pressure is important for the equilibrium, but the non-inductive current density calculations require the pressure to be separated into electron and ion density and temperature. This division is shown in Fig. 9 for the three gyrotron scenario with  $\beta_N = 4$ .

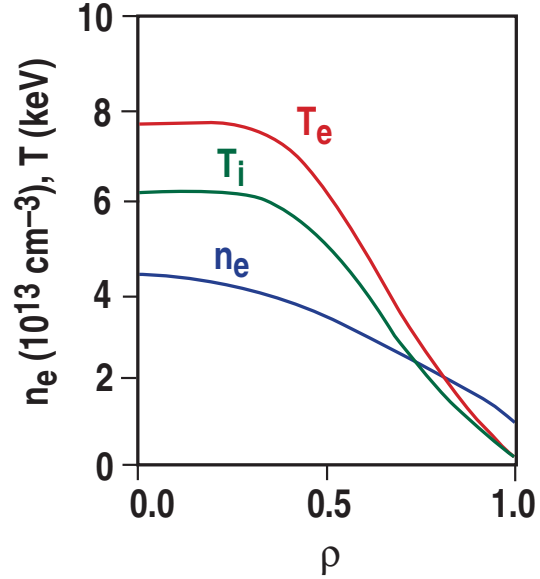


Fig. 9. NCS profiles of temperature and density.

The density profile was chosen to be consistent with pumped ELMing H-mode discharges at higher  $q_{95}$ . These are more peaked than the canonical H-mode density profiles normally shown. Very little effort was directed to make an H-mode edge pedestal or consistency between the edge bootstrap current density and the total current density from the equilibrium because the purpose was to show whether the off-axis ECCD was sufficient in these conditions. The lack of predictive capability of the edge conditions during ELMs would make any detailed reconciliation baseless in any case. The level of the line-averaged density was limited by the empirical rule-of-thumb on DIII-D that the ELMing H-mode density can be varied from  $n$  ( $10^{19} \text{ m}^{-3}$ ) = 3 I (MA) to 6 I (MA). The actual density was maximized consistent with full non-inductive current. The impurity density profile was chosen arbitrarily to give a constant  $Z_{\text{eff}} = 1.5$  across the plasma.

The temperature profiles were chosen to be a constant fixed ratio across the entire plasma. The transport code was run in analysis mode to derive both the local transport coefficients and the global confinement relative to the ITER-89P scaling law. The local transport coefficients were checked to ensure the ion diffusivity was at or above neoclassical and near the electron diffusivity.

The same source calculations in the transport code also provide the non-inductive current densities due to NBI, bootstrap, and ECCD. The scenario was iterated to give zero net ohmic current, not zero ohmic current density at all radii. Again, the goal of our modeling at that time can be seen directly by examining Fig. 10 which shows the total current density from the equilibrium and the non-inductive current densities calculated using the profiles in Fig. 9. It is clear that 2.3 MW of EC power delivered to the plasma under these conditions supplies sufficient current at the half radius to maintain the off-axis current density in conjunction with the bootstrap current. A resistive evolution could

have been done and would have resulted in a less reversed  $q$  profile, but the degree of negative central shear is not believed to be an essential feature of this scenario.

Fixing the profiles is obviously equivalent to fixing the target  $\beta_N$  and  $H$  factor for the scenario. These calculations do represent first principles evaluations of where to place the RFCD and the efficiency of the RFCD. These calculations are of value in determining the rf and NBI power levels needed to make the target scenario in terms of current drive and assuming the target values of  $\beta_N$  and  $H$ . Scenarios at increasing plasma current and field were developed.

Two scenarios are summarized in Table 3. We have labeled these scenarios by the number of gyrotron tubes we believe we will need to carry them out and also by the year in which we feel we can begin to attempt these scenarios. These scenario definitions have given focus to the effort in Thrust Area 2 in 1999 to develop transiently the plasma described in the year 2000 column. Good progress was made in 1999 on this scenario as shown in Fig. 11. This discharge is an ELMing H-mode as shown by the  $D_\alpha$  trace, Fig. 9(f). The discharge is quasi-stationary for  $\sim 2$  s or  $16 \tau_E$  and has a  $\beta_N H$  product of 9.  $\beta_N$  is just below 4 and is larger than the nominal no-wall limit of  $4 \times \ell_i$ , Fig. 11(c). Small recurring resistive wall modes were observed and are the cause of the periodic drops in  $\beta_N$ . The plasma described in the year 2001 column is our principal target for the year 2001 demonstration of a sustained NCS AT mode, possibly with an integrated divertor solution.

In order to obtain sufficient current drive efficiency, these scenarios use low densities, a low fraction of the Greenwald limit. These low densities are below where detached divertor plasmas are found, setting the challenge to either raise the scenario density or to the divertor program to develop ways of making radiative divertors compatible with these AT core plasmas. Density control at least is required from the divertor program to meet these scenarios.

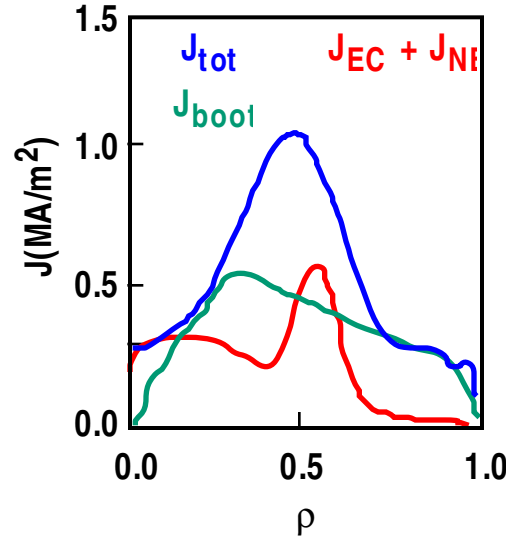


Fig. 10. Contributions to a hollow current profile.

**Table 3**  
**Parameters of NCS Scenarios Using Fixed Profiles.**

	4 Tubes (2000)	6 Tubes (2001)
$P_{EC}$ (MW)	2.3	4.5
$P_{FW}$ (MW)	3.6	3.6
$P_{NBI}$ (MW)	4.1	3.8
$I_p$ (MA)	1.0	1.3
$I_{Boot}$ (MA)	0.65	0.9
$I_{ECCD}$ (MA)	0.15	0.2
$B_T$ (T)	1.6	1.75
$\beta_T$ (%)	4.0	6.3
$\beta_N$	4.0	5.3
$H_{89P}$	2.8	3.5
$n$ ( $10^{20} \text{ m}^{-3}$ )	0.32	0.5
$n/n_G$	0.3	0.4
$T_i(0)$ (keV)	6	8
$T_e(0)$ (keV)	8	9

### 2.2.2 NCS Scenario Simulations Using Diffusion Coefficients Derived From Discharges

MHD stability studies of discharges with an internal transport barrier (ITB) show that the stability limit improves with increasing width and radius of the ITB based on a systematic scan of simulated equilibria with model  $q$  and pressure profiles. The scenario modeling described in the preceding section began with a total pressure profile consistent with an MHD stable equilibrium and rather arbitrarily divided the total pressure into electron and ion pressure which were then portioned to density and temperature. The scenario modeling described in this section is based on transport coefficients determined from an existing ITB discharge with an L-mode edge which are then scaled to different parameter regimes. To date the studies have been focused on using this approach to achieve the discharge conditions chosen by the method of the previous section.

Time-dependent transport simulations were performed using the ONETWO and CORSICA transport codes. First, measured profiles from an ITB discharge from our 1999 campaign, very similar to that shown in Fig. 11, with  $B_T = 1.6$  T,  $I_p = 1.2$  MA,  $q_{95} = 5$ ,  $\beta_N = 3.7$  and  $H_{89P} = 2.9$  were used to calculate thermal diffusivities  $\chi_e(\rho)$  and  $\chi_i(\rho)$ . These calculated diffusivities, with the addition of the ion neoclassical diffusivity shown in Fig. 12, were the baseline model diffusivities used in the time-dependent ONETWO simulations. The target parameters for the simulations are exactly those of the ITB

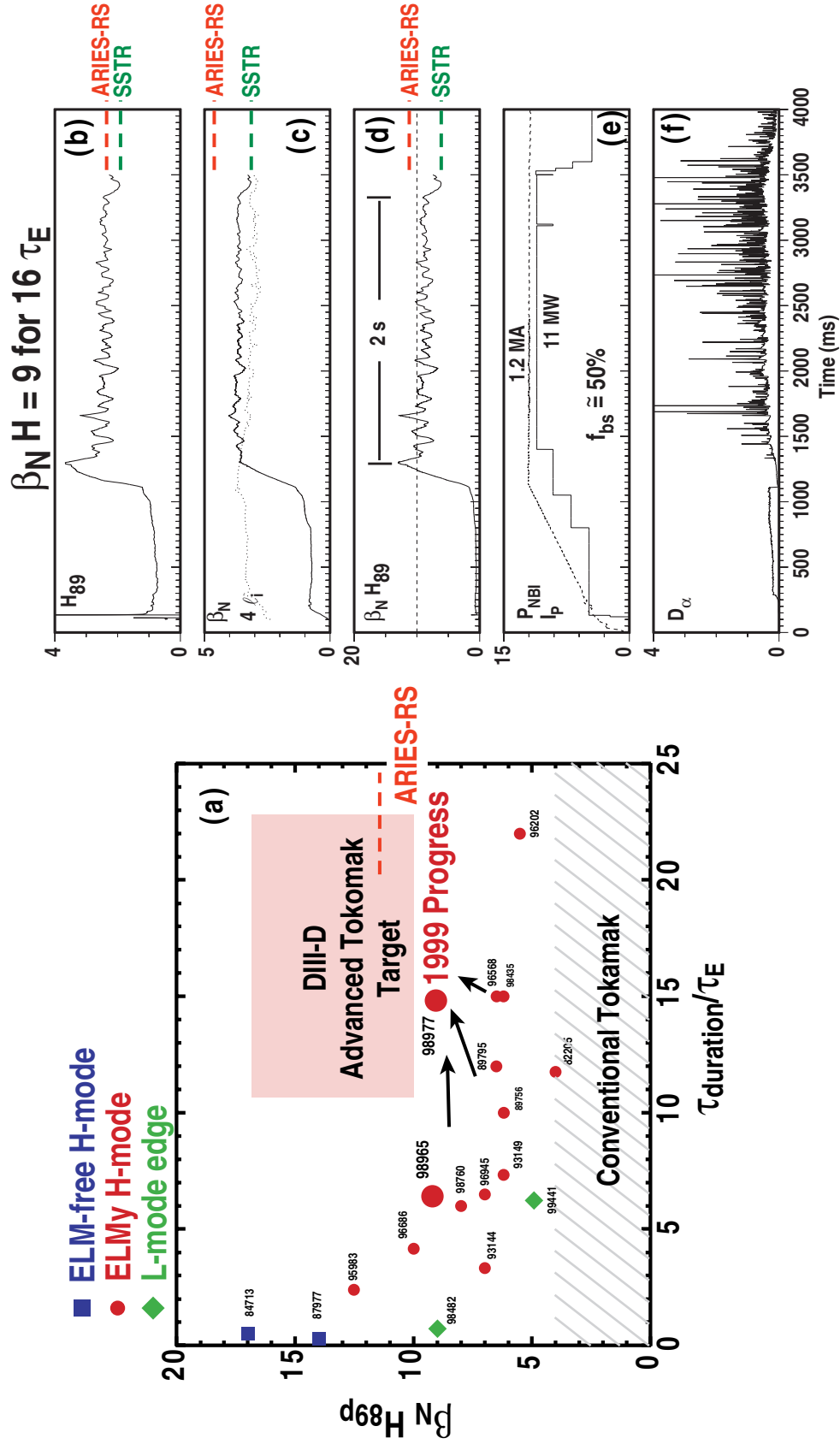


Fig. 11. (a) Recent progress in AT scenario development. Two large circles are 1999 results. (b) Confinement enhancement,  $H_{89p}$ ; (c) normalized beta,  $\beta_N$  (solid) and 4 x internal inductance,  $\ell_i$ ; (d) product  $\beta_N$ ,  $H_{89p}$ ; (e) beam power (solid), plasma current (dashed); (f) divertor  $D_\alpha$ .

discharge. CORSICA simulations have concentrated mostly on the sensitivity of results to other transport models.

In the process of performing the transport simulations, a number of iterations are carried out in order to optimize various choices. The ECH launching direction is optimized to align the electron cyclotron current drive (ECCD) profile with the off-axis bootstrap current profile, and to maximize the ECCD efficiency to overcome the dissipating ohmic current profile. We then evolve  $T_e$ ,  $T_i$ , and current density with a fixed density profile for a period of 10 s. The transport profiles ( $\chi_e$ ,  $\chi_i$ ) remain fixed to those from the experiment. We iterate this transport simulation cycle three times, each with the starting profiles taken from those at the end of the previous cycle. In the last cycle, evolution of the MHD equilibrium is also performed. At the end of each cycle, we test the MHD stability with high- $n$  (BALOO code) and low- $n$  (GATO code) stability.

Figure 12 shows the summary of simulations for  $q(\rho)$ ,  $T_e(\rho)$ ,  $T_i(\rho)$ , and individual components of the current density profile together with a tabulation of the parameters

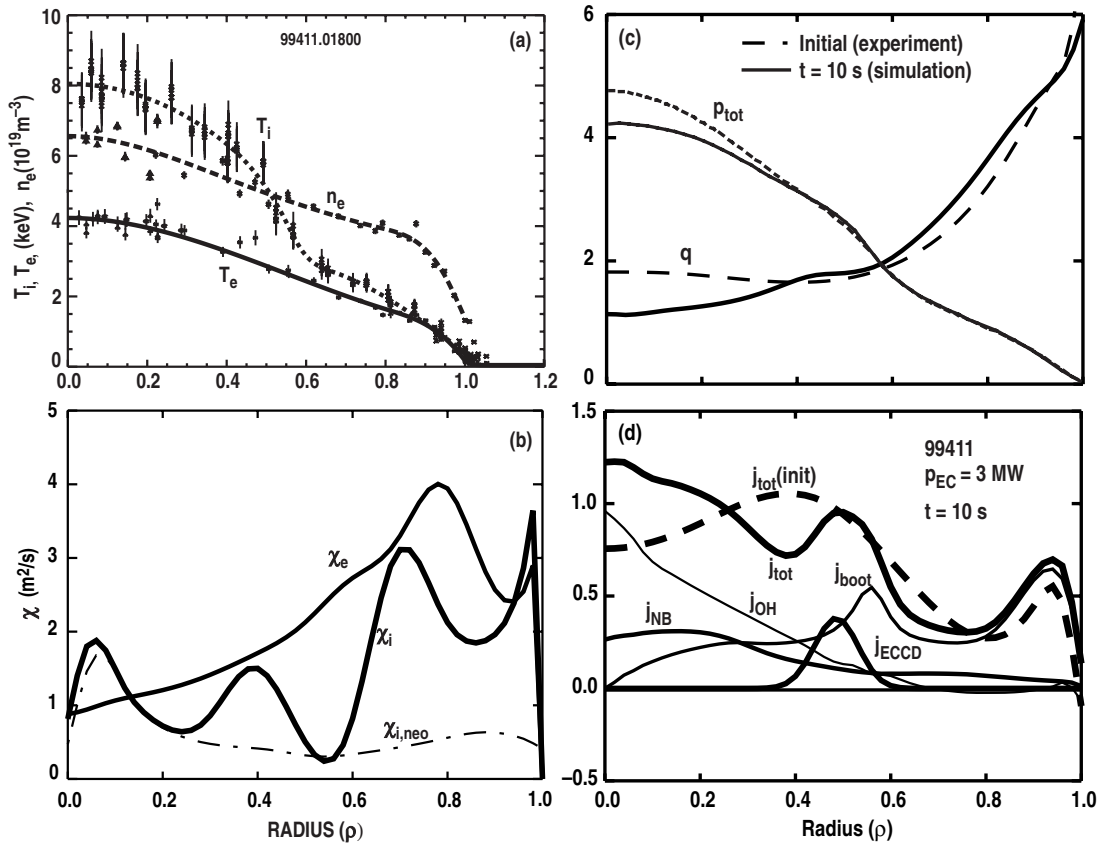


Fig. 12. NCS scenario using empirical transport coefficients. (a) Measured ion temperature, electron temperature, electron density; (b) experimental thermal diffusivities; (c)  $q$  profile, total pressure; (d) current profiles.



(Table 4), which can be compared with the case from the previous section. The detailed case shown in Fig. 12, illustrates that 3 MW of off-axis ECCD at  $\rho = 0.5$  maintains  $q_0 > 1$  and weak shear for 10 s and, we expect, sustains the high performance phase, allowing more detailed evaluation of AT physics. With the addition of density control with the two upper cryopumps, we expect significantly more electron cyclotron current and expect a quasi-stationary current profile.

**Table 4**  
**Parameters of L-Mode Edge NCS Scenarios Using Transport Simulations**

	4 Tubes (2000)
$P_{EC}$ (MW)	0→3.0
$P_{FW}$ (MW)	0
$P_{NBI}$ (MW)	9.2→6.2
$I_p$ (MA)	1.2
$I_{Boot}$ (MA)	0.67
$I_{ECCD}$ (MA)	0.9
$I_{OH}$ (MA)	0.24
$B_T$ (T)	1.6
$\beta_T$ (%)	4.3
$\beta_N$ (%)	3.7→3.5
$H_{89P}$	2.9→2.6
$n$ ( $10^{20} \text{ m}^{-3}$ )	0.48
$n/n_G$	0.48
$T_i(0)$ (keV)	8.4→6.9
$T_e(0)$ (keV)	4.2→4.5
$q_{95}$	5.0
$J_{BS}$	55%

### 2.2.3 NCS Scenarios Using Models of Transport Barrier Formation

Scenarios using models of transport barrier formation have been produced twice. A table of numbers for these scenarios is given in Table 5. These scenarios were constructed by 1-D simulations using the ONETWO code. All of the scenarios lie in the range  $\beta_T$  5%–11% at full field in DIII-D. They are at plasma currents of 1.6–2.2 MA and employ strong shaping ( $\kappa = 2.1$ ,  $\delta = 0.8$ ). They employ a total of 15–20 MW of total heating and/or current drive power, made up of roughly equal contributions of NBI, ECH, and FW. They all employ fast wave heating to achieve a high core electron temperature.

**Table 5**  
**Parameters of Longer Range DIII-D Scenarios**

Case	1	2	3	4	5
$\beta$ (%)	7.5	5.0	8.1	8.7	11.5
$\beta_N$	5.7	3.8	6.2	5.8	6.0
$I_p$ (MA)	1.6	1.6	1.6	1.8	2.2
$I_{bootstrap}$	1.07	1.45	1.85	1.92	2.1
$I_{ECCD}$	0.35	0.50	0.03	0	0
$I_{FWCD}$	0	0	0	0	0
$I_{NBCD}$	0.25	0.11	0	0	0
$I_{OH}$	-0.07	-0.46	-0.28	-0.12	-0.10
$q_{95}$	6.5	5.0	5.0	5.3	3.6
$q_0$	3.8	2.3	2.5	3.9	3.4
$q_{min}$	2.6	3.3	2.1	2.3	
$T_i(0)$ keV	15	12.3	18.5	14.5	19
$T_e(0)$ keV	8.5	9.7	7.0	12.7	13
$n_e(0)$ $10^{20} \text{ m}^{-3}$		0.59	0.89	0.72	0.88
$\bar{n}$ $10^{20} \text{ m}^{-3}$	0.57	0.35	0.54	0.48	0.53
$n_{edge}$ $10^{20} \text{ m}^{-3}$		0.23	0.23	0.23	0.21
$\bar{n}/n_G$	0.4	0.26	0.4	0.32	0.3
P (MW)	20	14	12	14	14
$P_{NBI}$ (MW)	6.5	4.0	4.0	4.0	4.0
$P_{EC}$ (MW)	7.0	6.0	4.0	6.0	6.0
$P_{FW}$ (MW)	6.5	4.0	4.0	4.0	4.0
W (MJ)		1.25	1.3	4.6	6.0
$\tau_E$ (s)		0.21	0.29	0.28	0.4
$H_{89P}$	3.5	3.4	4.4	4.0	4.95
$\rho_{*e}$ at $\bar{T}_e$	$2.3 \times 10^{-4}$	$2.5 \times 10^{-4}$	$2.1 \times 10^{-4}$	$2.8 \times 10^{-4}$	$2.9 \times 10^{-4}$
$\rho_{*i}$ at $\bar{T}_i$	$1.3 \times 10^{-2}$	$1.2 \times 10^{-2}$	$1.5 \times 10^{-2}$	$1.3 \times 10^{-2}$	$1.5 \times 10^{-2}$
$v_{*e}$ at $\bar{T}_e$	$1.2 \times 10^{-2}$	$4.2 \times 10^{-3}$	$8.0 \times 10^{-3}$	$2.9 \times 10^{-3}$	$2.1 \times 10^{-3}$
$v_{*i}$ at $\bar{T}_i$	$2.7 \times 10^{-3}$	$1.8 \times 10^{-3}$	$0.8 \times 10^{-3}$	$1.6 \times 10^{-3}$	$0.7 \times 10^{-3}$

Case 1: SSC-VH [Turnbull PRL 74, 718 (1995)]

Case 2:  $\beta = 5\%$ ,  $P = 16$  MW,  $n$  &  $v_\phi$  transported

Case 3:  $\beta = 8\%$ ,  $P = 15.2$  MW,  $n$  &  $v_\phi$  transported

Case 4:  $\beta = 8\%$ ,  $P = 17$  MW

Case 5:  $\beta = 11\%$ ,  $P = 17$  MW

Except for Case 2, all these cases require at least 6 MW EC power delivered to the plasma. These considerations lead us to believe that a 10 gyrotron EC system will ultimately be needed to form the NCS plasmas at full field and current in DIII-D.

They all seek steady-state negative central shear current profiles for stability at high  $\beta_N$ . They also seek high bootstrap fractions and make up any difference in the plasma current and the bootstrap current by use of RF current drive. The resulting plasmas have rather low  $\rho_*$  and very low  $v_*$ , but they match up well along dimensionless parameter scaling paths to future tokamak devices (Section 2.4 of the Five-Year Plan). The scenarios all have rather low densities and high temperatures. The combination of low density (well below the Greenwald limit) and high power will make it particularly challenging to obtain radiating, detached divertors in these scenarios.

For reference, the first scenario is that published by (Turnbull, 1995, see also St. John IAEA 1994 and Taylor EPS 1994). At that time, DIII-D had seen plasmas with hollow current profiles, very high central betas (calculated to be second stable) and had also seen in other discharges the VH-mode, a transport barrier formed around  $\rho = 0.8$ . The scenario described considered combining these two features into what was called then Second Stable Core VH-Mode (SSC-VH). The inverted  $q$  profile and suitably broad pressure profile was shown through stability calculations to give  $\beta_N$  of 5.7 assuming wall stabilization. Various transport models were used for the electrons including INTOR scaling, the Rebut-Lallia-Watkins model and the Hsieh model for electrons. Essentially the ion diffusivity was taken to be neoclassical near the core (the transport barrier model here was a small multiplier times neoclassical ion transport inside the radius of  $q_{\min}$ ) and rising to 5 times neoclassical near the edge. A combination of bootstrap current which peaked off axis and off-axis ECCD were used to sustain the hollow current profile. On-axis NBCD was used to control the central current density. Fast Wave heating sustained the core electron temperature. A limitation of this scenario was the use of a fixed density profile; no density transport was considered. The rather broad density profile used still contributed a significant bootstrap current. Steady-state solutions were found with the required current profiles and pressure profiles for the high values of  $\beta_N$  in this scenario.

For the Five-Year Plan, we constructed transport simulations using a full but complex model of  $E \times B$  shear stabilization of turbulence to dynamically form the transport barrier in the simulation. The current profile was evolved to steady state verifying the compatibility of the transport barrier with the second stable core. The model is diagrammed in Fig. 2.3-1 on page 2.3-4 of the Five-Year Program Plan. The model calculates the turbulence shearing rate with no free parameters from the Hahm-Burrell formula based on the evolving density, temperature and rotation speed profiles. Then the local value of  $\omega_{E \times B}$  is compared to a model of the turbulence growth rate. This prescription for  $E \times B$  shear suppression is based on gyrofluid turbulence simulations of

Waltz, 1994. The location where the transport barrier forms depends upon both the growth rate profile (which tends to rise from the center) and the source (heating, momentum and fueling) profiles. The barrier usually forms first at the edge due to the high power flux density and the strong density gradient (fueling). The H-mode edge can be suppressed (in the model) by a combination of high edge radiation and low recycling. We did so in order to concentrate on the core transport barrier properties and not on the more difficult to model edge L-H transition. A transport barrier then forms first in the core owing to the peaked heating and/or momentum sources. In the experiments, the reduction of the ITG mode growth rates due to hot ions and fast ion dilution have been found to aid internal transport barrier formation. The negative magnetic shear also eliminates MHD ballooning modes. Raising the power makes the internal transport barrier expand as the  $E \times B$  shear pushes out against the rising growth rate. This model of transport barrier formation contains many feedback loops, since the radial electric field depends on all the profiles, and a very rich set of anticipated phenomena. It is also hard to run since both the model growth rate and  $\omega_{E \times B}$  depend on local gradients.

The cases considered all model an L-mode edge. The transport barrier forms where the turbulence shearing rate from the radial electric field exceeds the local growth rate of the turbulence. When density transport is turned on, the strong local fueling source at the edge easily forms an edge transport barrier which can quickly lead to excessive edge pressure gradients. A large part of the NCS research thrust is aimed at controlling the edge pressure. To avoid this problem, we imposed a large edge growth rate to keep the edge in L-mode and fixed the edge density. The thrust to use an L-mode edge is one of DIII-D main AT thrusts but considering the high power flow through that edge, substantial mantle radiation or other means to suppress the L-H transition will have to be found. These are issues for future experimental and simulation work.

Despite the complexity of the model, the results in Table 5 represent another set of internally consistent numbers of target  $\beta_N$  and H factors with the required power levels and locations of current drive required to produce the necessary current profiles. The target  $\beta_N$  and H factors are large and represent ultimate goals for the DIII-D AT Program. Even with the high H factors, a 10 gyrotron system is needed and the total summed heating and current drive power of 20 MW will be a challenge to the divertor power handling capability in long pulse.

For the near term scenarios, perhaps some of the qualitative features seen in these transport barrier modeling efforts are worth noting. The density transport equation was turned on in Cases 2 and 3 and a transport barrier was allowed to form in the density channel (Fig. 13). Density gradients are more effective than temperature gradients in creating bootstrap current and for that reason, we obtain more bootstrap current than in the original SSC-VH scenario. Also, we have moved the transport barrier further out in

radius and that also increases the total bootstrap current. We find it rather easy (in fact too easy in these simulations) to obtain full bootstrap current. It appears that with central fueling from beams or pellets and a longer time for the density to accumulate, we should see strong transport barrier formation in the future through density gradient with accompanying large bootstrap fractions. This research area has only just started on DIII-D. We completed the central Thomson scattering system and it is now operational on DIII-D. With it we will finally be able to see what is happening in the density channel when transport barriers form in the plasma interior. The UCLA group installed an x-mode interferometer on DIII-D about a year ago so we could get an early glimpse of a density transport barrier. One such profile (Fig. 14) shows a spectacularly high density gradient, showing us what exciting phenomena may lie ahead in these studies. We have a plan in the 1999 campaign in the Thrust 7 on ITB control to use the inside launch pellet injection together with the counter beam injection to stimulate the formation of transport barriers in the density profile.

Another interesting but not fully understood result was that the ECH was very effective at moving the location of the transport barrier. To see such dynamics was a principal reason for using the complex  $E \times B$  shear model. The ECH deposition profile is about as narrow as the gradient regions of the transport barrier, and so the ECH is a precision tool

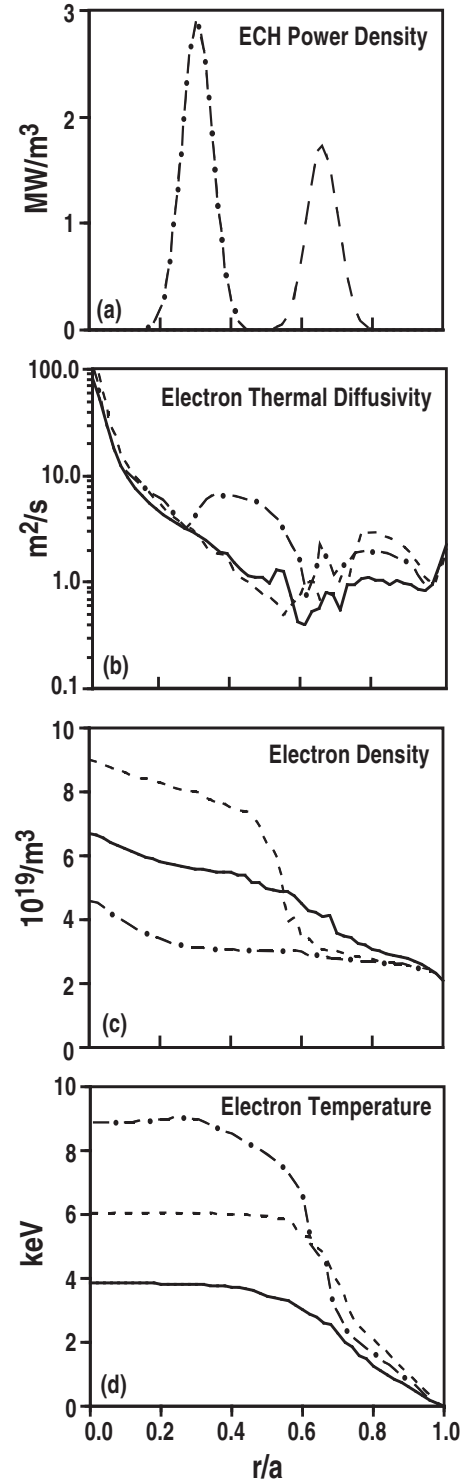


Fig. 13. ECH barrier control is illustrated by a three-case comparison: 6 MW NBI only (solid), 6 MW NBI + 6 MW ECH at  $r/a \sim 0.7$  (dashed), 6 MW NBI + 6 MW ECH at  $r/a \sim 0.3$  (dot dashed). Shown are profiles of (a) ECH power density, (b) model electron thermal diffusivity, (c) electron density, and (d) electron temperature.

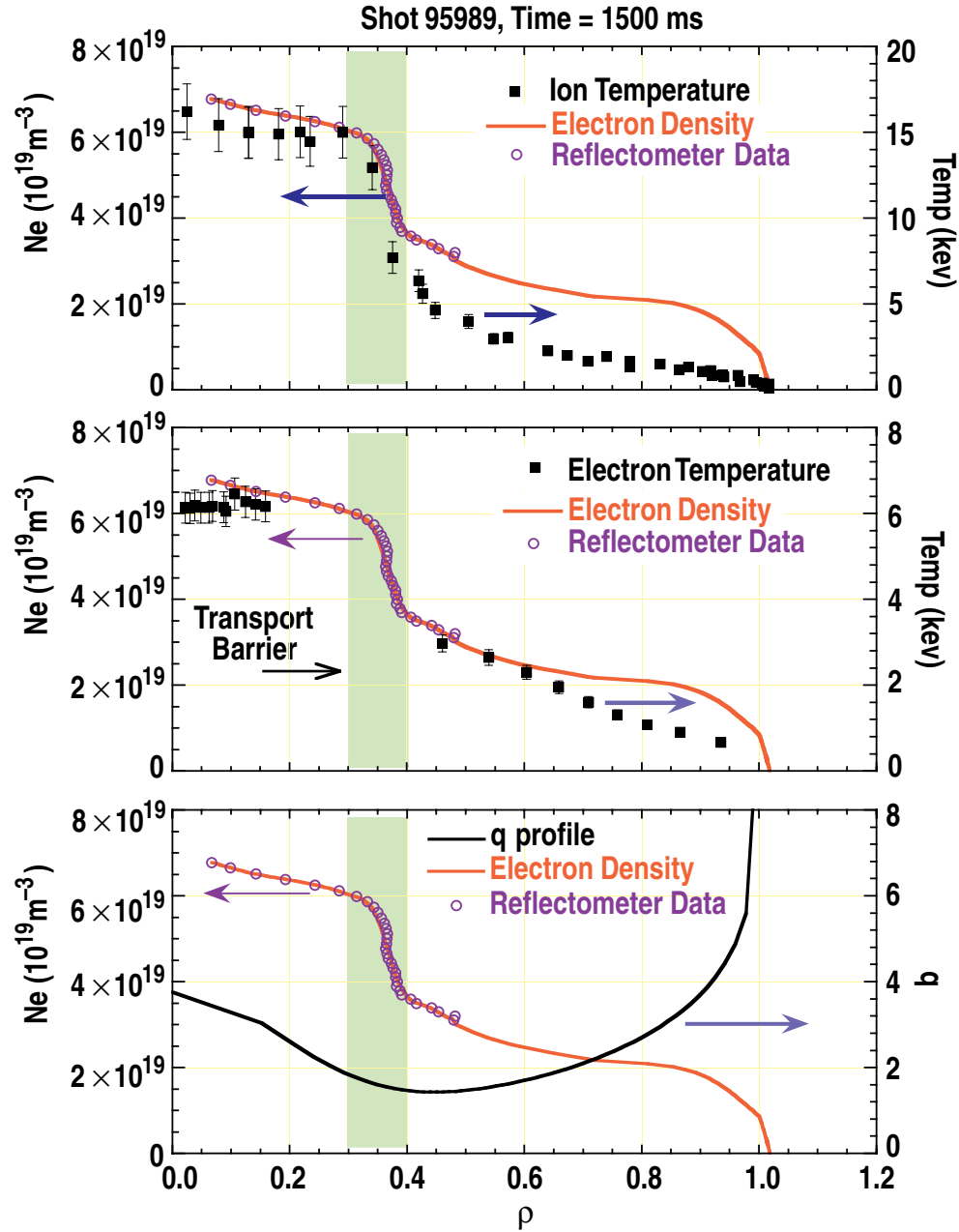


Fig. 14. Transport barrier in the density.

for barrier control. We found that ECH applied just outside the radius where a transport barrier was beginning to form would draw the transport barrier out to larger radius. Equally striking but not so positive was the effect of ECH when applied inside a formed transport barrier. The transport barrier was found to retreat to just inside of the ECH absorption layer. In the model this was due to the fact that the model growth rate increased with the electron temperature gradient but the  $E \times B$  shear only depends on the ion temperature gradient. Thus, electron heating caused a loss of the  $E \times B$  shear suppression. A retreat of an existing internal transport barrier with central ECH heating has been

observed on DIII-D. Linear growth rate calculations suggest that the excitation of electron temperature gradient modes may be the cause. These modes are not expected to be stabilized by  $E \times B$  shear since they have very large growth rates (and small wavelengths).

The physics picture mentioned above in which  $\omega_{E \times B}$  pushes out radially against a radially rising turbulence growth rate suggests that the way to move the transport barrier out in radius is just to add power or momentum inside the formed transport barrier. However, because the transport coefficients are so low inside the barrier, increasing the power, especially localized power, can produce wild swings in local gradients affecting not only  $\omega_{E \times B}$  but stability as well. The way through these complications is to increase power slowly. Using this approach, we were able in 1998 to make an internal transport barrier discharge that lasted the whole length of the neutral beam pulse (5 s). This was done at low current where the plasma was beset with Alfvén eigenmodes which had the beneficial effect of throwing out enough fast ions so that the central NBCD was weak and the central  $q$  stayed high. When such discharges were attempted at higher current, the Alfvén eigenmodes were eliminated but the central NBCD drove  $q_0$  below one and instabilities terminated the high performance phase.

In the 1999 Thrust 7 campaign, counter-NBI was used as a means to achieve near stationary  $q$  profiles with elevated  $q_0$  and to evaluate techniques to expand the ITB. With co-NBI, the sheared  $E_r$  from the plasma rotation and that from the pressure gradient are in opposition. This gives a sharp gradient in  $E_r$  (large local  $\omega_{E \times B}$ ) but the dynamics are such to make it difficult to increase the radius of the large local  $\omega_{E \times B}$ . In contrast, with counter-NBI, the  $E_r$  from the plasma rotation and the pressure gradient are additive. The local values of  $\omega_{E \times B}$  are not as large as for the co-NBI case, but as the beta increases, the region of large  $\omega_{E \times B}$  expands and the ITB with it.

The various cases have varying assumptions about how low the transport rates become inside the transport barrier. In DIII-D we have already seen ion neoclassical transport rates all across the cross section so this assumption for the residual transport was made in all cases. But it is clear that similarly low levels for transport rates for electrons and particles in DIII-D are too good. Beta limits would be quickly exceeded. DIII-D does not presently see as much transport reduction in the electron and particle channels as in the ions and apparently will not require it to reach the scenarios shown.

These are some of the interesting phenomena we have seen in our initial exploration of the possibilities for AT physics in the plasma core. The simulations presented give a feeling for the parameter regimes achievable, the power levels in various systems to achieve them, the density and edge control that may be required. But the main value of such simulations is to open a wide vista of new phenomena that should open up as the

auxiliary capabilities of DIII-D are developed toward the goal of long pulse sustainment of AT operating modes.

## 2.2.4. Recent ARIES-AT Scenarios

We have also explored optimization of AT scenarios as part of the ARIES-AT study. These studies have pushed conceptually and computationally closer to what might be the ultimate stability and transport potential of the tokamak. Here we have looked for pressure profiles consistent with very high bootstrap fractions ( $f_{BS} = I_{BS}/I_p > 0.9$ ) and high beta values (wall stabilized). Equilibria are found with  $\beta_N = 5.6$  (wall stabilized),  $q_{95} = 3.3$  and  $f_{BS} = 0.92$ , as shown in Fig. 15. The high fraction of bootstrap current at such a low  $q$  value is a consequence of the large value of  $q_{min} \sim 2.5$  and the large radius of  $q_{min}$ ,  $\rho_{q_{min}} \sim 0.8$ . The key physics to such a scenario is the ability to form and control a transport barrier at large radius,  $\rho_{ITB}$ ; with small gradients near the boundary. Analysis shows that sufficient sheared  $E \times B$  flows to stabilize ITG modes in such a plasma are feasible. Understanding and controlling shorter wavelength micro-instabilities remains a challenge. The ARIES-AT study clearly defines a challenging approach for the optimization of DIII-D NCS plasmas — expanding and controlling the transport barrier at large radius and this effort is the focus of Thrust 7.

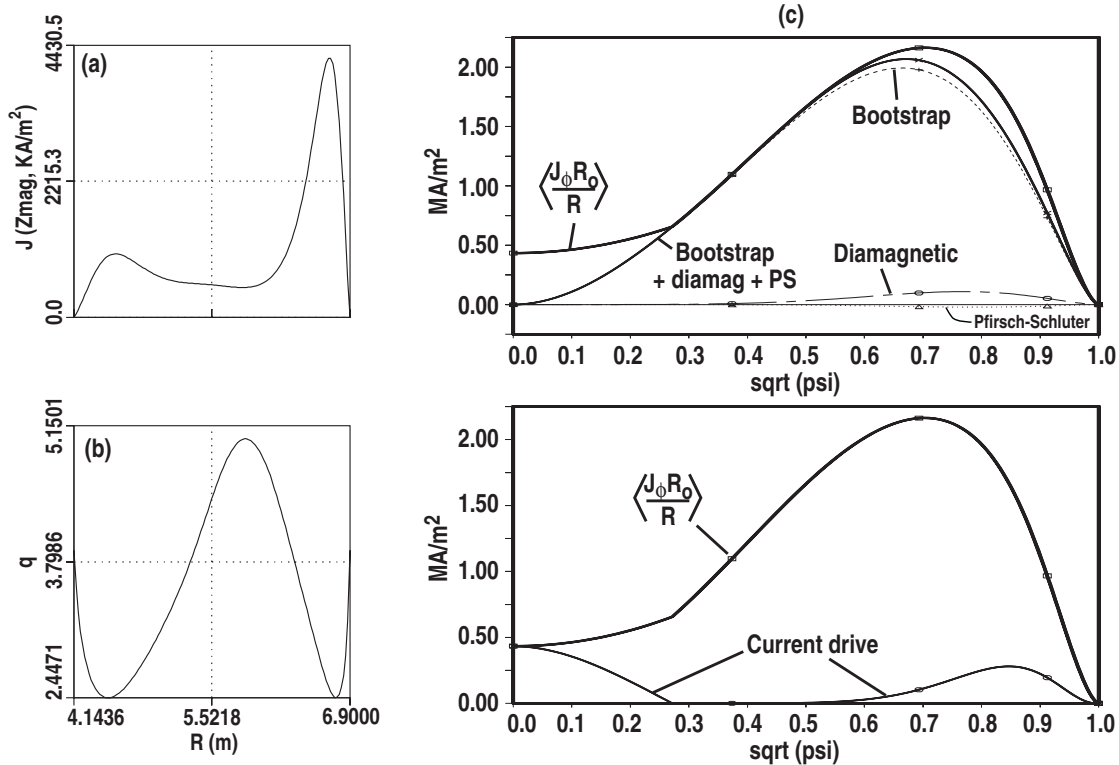


Fig. 15. High bootstrap fraction ARIES-AT scenario: (a) plasma current; (b)  $q$  profile; (c) total current (solid), bootstrap (dashed), and diamagnetic current (chain dashed).



### 2.3. THE HIGH INTERNAL INDUCTANCE SCENARIO IN DIII-D

The high internal inductance (high  $\ell_i$ ) scenario is the second possible approach to AT performance being pursued in DIII-D research. This scenario is motivated by the well-established experimental observation that both the beta limit and the confinement multiplier increase approximately linearly with  $\ell_i$ . This scenario has the advantages that the current and  $q$  profiles are monotonic, requiring less precise tailoring, that the current density and pressure gradient at the plasma edge are not so large as to require wall stabilization to reach  $\beta_N \approx 4$ , and that the required external current drive would be peaked at the axis which is more efficient and easier to implement than in the NCS scenario.

In order to achieve high values of  $\beta_N$ , relatively broad pressure profiles are required. This places the regions of high pressure gradient toward the discharge edge and, in discharges with large bootstrap current fraction, produces relatively broad current profiles. So, operation at high  $\beta_N$  and high bootstrap fraction tends to lower the self-consistent value of  $\ell_i$ .

The achievable value of  $\beta_N$  is expected to be consistent with the empirical scaling  $\text{Max}(\beta_N) \approx 4 \ell_i$ . Thus, a  $\beta_N \approx 4$  operating point would have  $\ell_i \approx 1$ , a larger value than in the NCS scenario but smaller than the maximum values achieved in previous research on  $\ell_i$  scaling. Simulations have shown that bootstrap fraction in the range 50%–70% can be obtained self-consistently with  $\ell_i \approx 1$ . A sample equilibrium of this class is shown in Fig. 16. With strong shaping ( $\delta \geq 0.7$ ) and flat  $J$  and  $q$  profiles in the center of the plasma, an optimized equilibrium can be found which is stable to  $n = 1$  ideal modes and to  $n = \infty$  ballooning at  $\beta_N = 4$  without a conducting wall. This case has not as yet been examined for transport requirements although the bootstrap current profile is required to be consistent with the assumed pressure profile.

The achievable value of  $\ell_i$  for a given bootstrap fraction can be increased by reducing the value of the safety factor on axis. Reducing  $q_0$  below 1 requires stabilization of the sawtooth instability. Previous work has indicated that sawtooth stabilization is possible with rf heating. A key question for the high  $\ell_i$  scenario is whether rf sawtooth stabilization can be done while maintaining the other requirements (high  $f_{BS}$  and  $\beta_N$ ). Note that sawtooth stabilization should remove a primary source of perturbations which can initiate neoclassical tearing modes, which in turn may raise the beta limit. An example of this scenario is shown in Fig. 17. This example was developed with the same rules as the NCS example cited in Section 2.2.1, i.e., primarily to assess heating and current drive requirements.

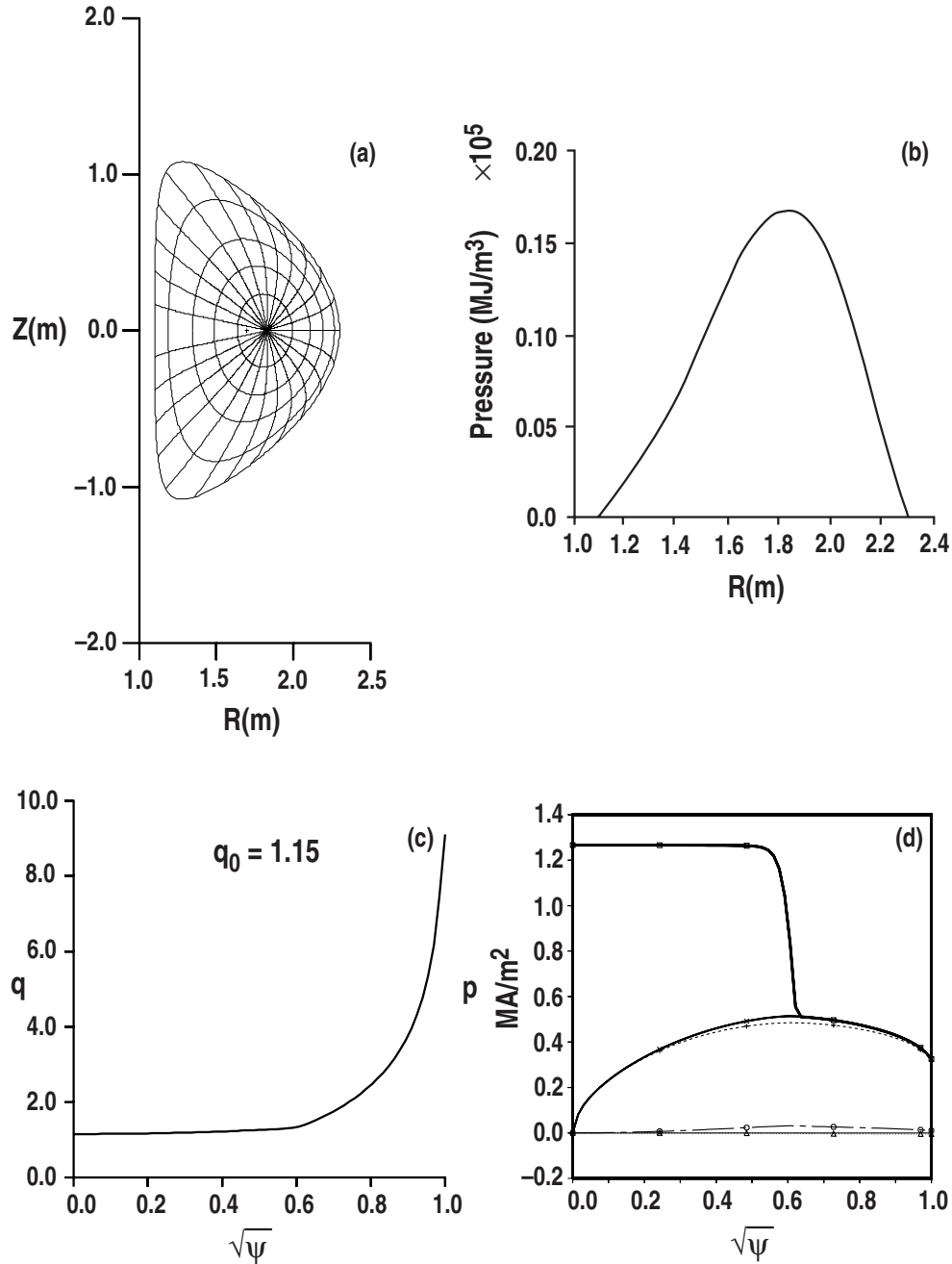


Fig. 16. Optimized  $\ell_i$ , high  $\beta_N$ , edge aligned bootstrap equilibrium in the full-size DIII-D configuration with  $R = 1.7$  m,  $a = 0.6$  m,  $\kappa = 1.8$ ,  $\delta = 0.7$ ,  $B = 1.9$  T,  $I_p = 1.1$  MA,  $q_0 = 1.15$ ,  $\ell_i = 0.92$ ,  $p_0/\langle p \rangle \sim 3.0$ ,  $\beta_N = 4.0$ , and  $f_{BS} = 70$ ,  $q_{95} = 6.5$ . (a) Flux contours, (b) pressure profile across the midplane as a function of major radius, (c)  $q$  profile as a function of  $\sqrt{\psi}$ , and (d) flux surface averaged toroidal current densities as function of  $\sqrt{\psi}$ . Here, solid squares represent the total plasma current. The sum of bootstrap (dotted curve), diamagnetic (open circles), and Pfirsch-Schluter (open triangles) contributions is represented by crosses. Comparison: 6 MW NBI only (solid), 6 MW NBI + 6 MW ECH at  $r/a \sim 0.7$  (dashed), 6 MW NBI + 6 MW ECH at  $r/a \sim 0.3$  (dot dashed). Shown are profiles of (a) ECH power density, (b) model electron thermal diffusivity, (c) electron density, and (d) electron temperature.

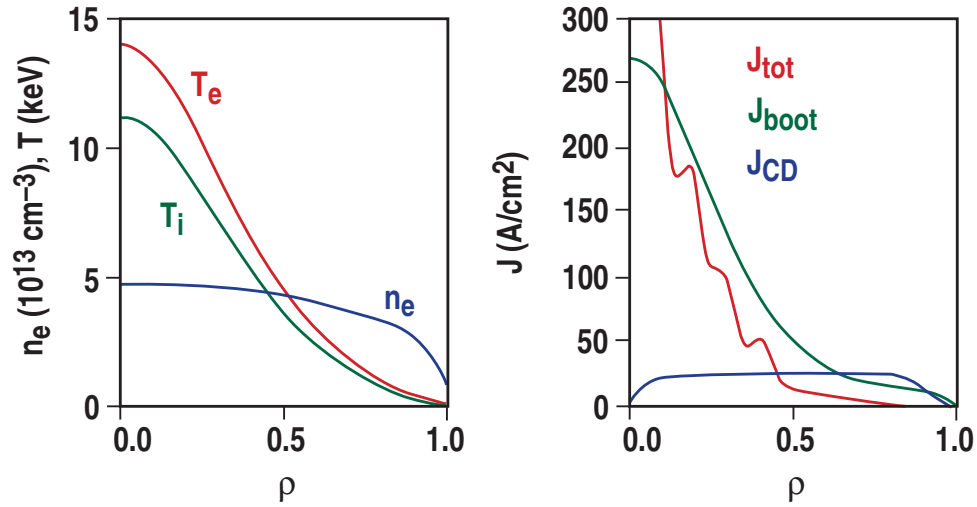


Fig. 17. A high  $\ell_i$  steady-state with  $\beta_N H > 10$  can be sustained by a 3 MW ECH system. The parameters are:  $B = 1.9 \text{ T}$ ,  $\ell_i = 1.6$ ,  $\beta_N = 2.5$ ,  $I_{BS} = 0.41 \text{ MA}$ ,  $I = 1.0 \text{ MA}$ ,  $\beta_N = 4.0$ ,  $P_{FW} = 3.6 \text{ MW}$ ,  $I_{FW3} = 0.17 \text{ MA}$ ,  $q_0 = 0.55$ ,  $H = 3.0$ ,  $P_{EC} = 2.4 \text{ MW}$ ,  $I_{EC} = 0.14 \text{ MA}$ ,  $q_{95} = 5.6$ ,  $n = 4.2 \times 10^{13} \text{ m}^{-3}$ ,  $P_{NB} = 5.0 \text{ MW}$ ,  $I_{NB} = 0.27 \text{ MA}$ .

Thus there are two distinct versions of the “high  $\ell_i$ ” scenario, one requiring some current profile tailoring to maintain  $q_0$  above 1 and sufficiently flat in the central region, and the other requiring effective stabilization of sawteeth.

One criticism of the high  $\ell_i$  scenarios has been that excessive external current drive power would be needed in a reactor. To examine this question explicitly, we have looked at spreadsheet modeling of three high  $\ell_i$  cases and compared them with ARIES-RS. Fixed parameters (with Aries-RS values in parentheses) are  $R = 5.0 \text{ (5.52) m}$ ,  $a = 1.8 \text{ (1.38) m}$ ,  $\kappa = 1.8 \text{ (1.7)}$ ,  $\delta = 0.7 \text{ (0.5)}$ ,  $q_{95} = 6.5 \text{ (3.5)}$ ,  $P_{\text{fusion}} = 2500 \text{ (2167) MW}$ , and  $n/n_{\text{Greenwald}} = 0.95 \text{ (1.78)}$ . Some of the results are summarized below.

	$\ell_i = 1$	$\ell_i = 1.25$	$\ell_i = 1.5$	ARIES-RS ( $\ell_i = 0.42$ )
$\beta_N$	4	5	6	4.84
$q_0$	1.15	0.85	0.55	2.78
$B \text{ (T)}$	7.5	6.58	5.95	7.98
$I \text{ (MA)}$	15	13.15	11.9	11.3
$f_{bs}$	0.61	0.67	0.60	0.88
$P_{CD} \text{ (MW)}$	169	126	123	81
$H_{89P}$	2.1	2.44	2.65	2.35

The benefits of high  $\ell_i$  operation are clear. If satisfactory sawtooth suppression is possible and the increase in  $\beta_N$  can be demonstrated, the  $q_0 = 0.55$  case has significantly lower magnetic field than ARIES-RS, with roughly the same total current. Although the driven current fraction increases by 233%, from 0.12 to 0.40, the required external power increases by only 52%. This is because the current is driven at the axis, where  $T_e$  is high and trapping is small making the current drive much more efficient. Further, because the current is driven at the axis, a less complex profile control system is needed.

The multi-year goal of research for the high  $\ell_i$  operating mode is to determine feasible scenarios for steady-state high  $\ell_i$  discharges in DIII-D consistent with the available tokamak resources. A goal would be to maintain elevated  $\ell_i$  values for twice the inductive decay time and confirm that the corresponding increase in confinement and stability is also maintained. The issues to be resolved over several years of work are:

1. Establish whether sawtooth stabilization is both possible and practical.
2. Establish the practical limits to  $\beta_N$  in the two high  $\ell_i$  scenarios without additional wall stabilization. Do the linear relationships between  $\beta_N$  and  $\ell_i$ , and between  $H$  and  $\ell_i$  extend to  $q_0 < 1$  cases?
3. Establish the current drive requirements for steady-state sustainment of these two scenarios. How much current profile control is needed for the  $q_0 > 1$  case?
4. Development of entirely self-consistent scenarios to find the optimum combination of current, density, and temperature profiles.
5. Select the  $q_0 > 1$  or the  $q_0 < 1$  approach.

Regrettably, due to the intense competition for run time on DIII-D, we do not anticipate being able to allocate run-time to this research thrust until 2002.

To outline the possible content of a future plan to pursue the high  $\ell_i$  scenario, we list here a simplified three-year view of the necessary research:

Goal:  $\beta_N \bullet H_{89P} > 10$  with no inductive flux

#### Year 1

Demonstrate sawtooth stabilization for  $>1$  s and validate the stabilization model. This includes modification and commissioning the ABB transmitters for operation at 60 MHz.

Develop the 3 MW ECH target scenario with  $\beta_N \bullet H_{89P} > 10$  transiently. This includes FW coupling studies under the appropriate edge conditions and identification of core pressure limits.

### Year 2

Demonstrate the 3 MW ECH integrated scenario. Develop a 6 MW ECH target scenario.

### Year 3

Demonstrate the 6 MW ECH integrated scenario. Develop a 10 MW ECH target scenario.

## **2.4. RESEARCH THRUSTS — THREE-YEAR VIEWS**

### **2.4.1. Edge Stability, Research Thrust 1 (Leader: J.R. Ferron, Deputy: L.L. Lao)**

This thrust is aimed at solving a key problem in improving steady-state performance in DIII-D AT regimes: the termination of the AT high performance phase by instabilities that originate in the plasma edge. Previously, DIII-D discharges have been produced with transient phases with very high values of normalized beta,  $\beta_N$  and confinement factor  $H$ . Values of the performance product  $\beta_N H_{89P}$  as high as 20 have been obtained, where  $H_{89P}$  is the performance enhancement relative to L-mode. During 1999, longer duration high performance phases were produced at reduced plasma current and toroidal field. For example, a relatively long duration discharge with  $\beta_N H_{89P} = 9$  lasted for approximately 2 seconds. While these values show great promise for the tokamak in its AT regimes, edge localized modes (ELMs) remain as an important limiting factor. This thrust is aimed at finding ways to stabilize these modes or to reduce their impact on the discharge performance.

Edge localized modes result from the large pressure gradient associated with the edge-localized transport barrier in H-mode. Large pressure gradients lead to significant bootstrap current being driven in the edge plasma. In shaped plasmas, this bootstrap current can open an edge-localized region with access to the ballooning mode second regime of stability. This enables the pressure gradient to increase above the calculated first ballooning regime limit. In this way a positive feedback loop is established between the edge pressure gradient, edge bootstrap current and the ballooning stability boundaries. Calculations and experimental results show that these conditions result in destabilization of low toroidal mode number coupled kink/ballooning modes. As a result of the low toroidal mode number, the radial extent of the unstable mode and the perturbation on the discharge can be significant. These instabilities serve as “soft” beta limits in that they cause a transition from an AT regime to an ordinary ELMy H-mode discharge.

We have shown that by closing access to the ballooning second stability regime, the positive feedback loop between the edge pressure gradient and edge current can be stabilized, resulting in less perturbing ELMs. However the increased edge pressure gradients allowed by second stable regime access also increase the edge pressure pedestal height and the overall confinement of the discharge. So, some compromise must be found between having the high edge pressure gradients and incurring instabilities severe enough to terminate the AT phase. It is the purpose of this thrust to find that balance.

Two approaches were explored in 1999. The first approach was to suppress second stable access in the edge region by choice of plasma shaping, seeking to build a high quality transport barrier inside the sufficiently stable, rapidly ELMing first regime edge plasma. Previous experiments had already shown that second regime access can be eliminated by either high or low squareness shaping of the discharge. In these experiments, an internal transport barrier was produced, but the results were dominated by locked modes apparently unrelated to ELMs. Further analysis of these results is required.

The second approach sought to retain the advantage in H-factor that results from edge region second stable regime access but to prevent or limit the consequences of the edge instabilities. Two approaches were planned. First, the growth of the edge pressure gradient (and therefore the resulting bootstrap current) was modified by impurity mantle radiation in order to keep the pressure gradient from reaching the unstable limit. These experiments were successful in preventing the occurrence of ELMs but the discharges suffered from a radiative collapse resulting from buildup of the injected impurity. In the second approach the plan was to use edge-localized ECH to decrease the edge collisionality. The idea was to increase the ratio of bootstrap current to pressure gradient in order to increase the size of the region with ballooning mode second stable regime access. These experiments were ultimately postponed because of ECH availability. In other experiments, the triggering of ELMs by injection of deuterium pellets was studied. These experiments produced interesting data on the instability threshold as a function of pressure gradient and edge pedestal width. Finally, discharges useful for understanding edge instabilities were produced as part of the Thrust 2 effort. These discharges had relatively high performance during the initial portion of the ELMing phase. Analysis is required to understand why good performance was maintained during ELMs in these discharges in contrast to what is normally observed.

The focus during 2000 will be on analysis and developing a new lithium beam edge current density diagnostic. Data obtained during 1999 will be compared with theory to improve our understanding of the physics of edge stability. Extensions to the GATO code allowing analysis of higher toroidal mode numbers ( $6 \leq n \leq 10$ ), and the ELITE code, which can evaluate stability of medium  $n$  coupled peeling/ballooning modes, will be utilized. One focus of analysis will be the relatively steady-state, high performance

ELMing discharges developed as part of Thrust 2 during 1999 to understand why the impact of ELMs on these discharges seems to be reduced.

One experiment on edge stability is planned for 2000 within the stability topical area to follow up on the results with impurity radiation by utilizing the RDP pump to control the impurity density. Finally, development of a diagnostic for improved measurement of the current density in the edge region is planned for 2000.

During 2001 and 2002, experiments on edge stability will resume. With the availability of improved edge current density measurements more accurate comparison of new experimental results with theory will be possible. Possible methods to modify the edge stability will be explored. Proposals that already exist include ECH in the edge region, various shape variations including a localized bump in the outer flux surface at the mid-plane to affect second stable regime access, and continuation of the use of impurity radiation and pellet injection. These experiments will follow up on the experiments that were begun during 1999. New experiments to make detailed comparisons to theory are planned, for instance the study of ELMs during limiter H-mode discharges for comparison with the theory implemented in the ELITE code. Experimental proposals generated during the 2000 year of analysis will also be explored.

#### **2.4.2. AT Scenario, Thrust 2 (Leader: T.C. Luce, Deputy: M.R. Wade)**

##### **Three-Year Goal**

Demonstrate normalized tokamak performance more than twice that of conventional ELMing H-mode with no inductive flux for a duration limited only by hardware constraints.

Goal:  $\beta_N \cdot H_{9P} > 10$  with no inductive flux.

##### Critical Path Items

##### **Tool Development.**

- Gyrotron commissioning (up to six gyrotrons operational)
- EC launcher commissioning
- Validation of ECCD in ELMing H-mode plasmas
- Particle (density) control
- Feedback control with the PCS

##### **Physics Issues.**

- Assessment of effects of  $q_{\min}$  and  $q_{95}$  on bootstrap current fraction and alignment.
- Assessment of confinement when  $T_e$  approaches  $T_i$ .

Assessment of impurity accumulation.

Assessment of resistive wall mode avoidance and suppression techniques.

### Draft Three-Year Outline Plan

#### **Issues to Address in 2000.**

- Apply new RDP hardware for particle control.
- Commission new gyrotrons and new launchers.
- Validate ECCD in ELMing H-mode.
- Demonstrate PCS real-time q profile measurement.
- Assess impact on confinement of  $T_e$  approaching  $T_i$ .
- Assess difficulty in extrapolating performance to higher I, B.

#### **Issues to Address in 2001.**

- Demonstrate 3 MW ECH integrated solution.
- Develop 6 MW ECH target scenario.
- Commission 6 MW system.

#### **Issues to Address in 2002.**

- Demonstrate 6 MW ECH integrated solution.
- Establish basis for extrapolation.
- Develop 10 MW ECH target scenario.

### **2.4.3 Neoclassical Tearing Mode, Thrust 3 (Leader: R.J. La Haye, Deputy: C.C. Petty)**

Two principal research lines are foreseen in a three year plan: (1) studies in H-mode with sawteeth present and (2) studies in an AT mode with raised  $q_{\min}$  (Fig. 18).

#### **H-Mode With Sawteeth**

##### 2000

Reduce the width of the 3/2 mode with ECCD.

Test physics of polarization threshold.

##### 2001

Shrink the modes and/or prevent their onset with ECCD.

##### 2002

Suppress the 3/2 and/or 2/1 modes separately using two ECCD systems.



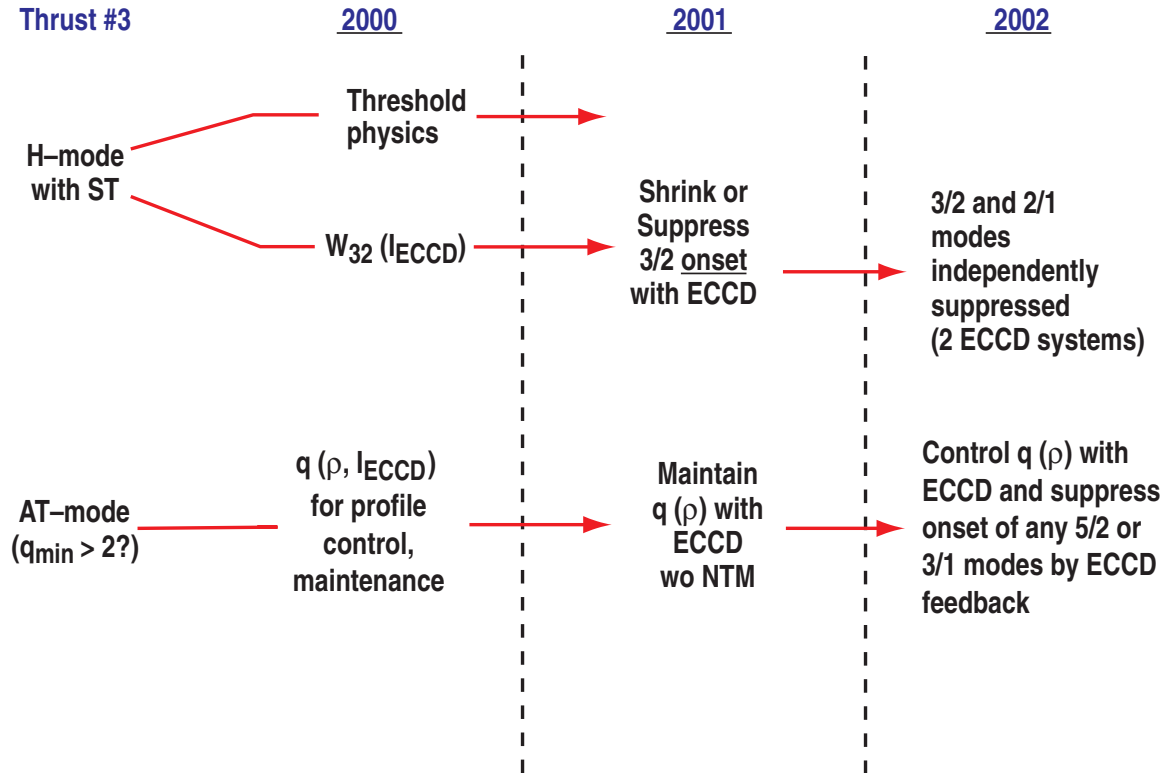


Fig. 18. NTM Research Plan.

**AT Mode Line**2000

Study the variation of the  $q$  profile with ECCD.

2001

Maintain the  $q$  profile with ECCD so as to avoid NTM onset.

2002

Control the  $q$  profile and suppress any 5/2 and/or 3/1 modes by 2 ECCD systems.

**2.4.4. Wall Stabilization, Thrust 4 (Leader: G.A. Navratil, Deputies: A.M. Garofalo, M. Okabayashi)**

Validate the model of wall stabilization and begin feedback stabilization experiments.

Overall Goal: Sustained operation at beta significantly above the no-wall limit.

Progress in 1999: Validate Models of Rotational Stabilization and Initial Experiments on Feedback Control

**Physics of Wall Stabilization and Plasma Rotation.**

- Three AT plasmas were developed for RWM Study: SND ( $\beta_N^{\text{no-wall}} \sim 2$ ); DND ( $q_{95} \sim 4.5$ ); DND ( $q_{95} \sim 5.5$ ; record long pulse  $\beta_{NH} \sim 9$ )
- The  $n=1$  RWM limits the performance of low- $\ell_i$  AT plasmas to  $\beta_N \leq 4\ell_i$ .
- Plasma rotation unable to completely suppress RWM for  $\beta_N \geq 4\ell_i$ .
- Plasma toroidal rotation strongly reduced whenever detectable RWM is present ( $\delta B_r \geq 1$  Gauss).
- Test of  $q_{\min}$  dependence of rotation threshold inconclusive: unable to vary  $q_{\min}$  above and below 2 at RWM onset time.
- RWM “bursting” observed in DND plasmas near  $\beta_N^{\text{no-wall}}$  limit.

**Initial Feedback Control Experiments (PoP Test).**

- Radial flux leakage of  $n=1$  mode through the vacuum vessel can be compensated by the feedback system: test of basic “Smart Shell” algorithm.
- Three feedback algorithms were tested: “Smart Shell”; “Fake Rotating Shell”; and “Mode Control”
- “Fake Rotating Shell”: co-injection direction favorable for stabilization.
- Smart shell control of low density locked mode was ineffective: tearing mode not sensitive to radial flux compensation on vacuum vessel wall.
- 3-D code VALEN improved to include GATO generated  $n=1$  RWM current distribution in the plasma model: basic tool for design of an optimal C-coil extension for mode control.
- 2-D simulation of active RWM control by A. Bondeson [MARS] and M. Chance/M. Chu [PEST-VACUUM] is in progress.

**Extend Lifetime of Plasma Above the No-Wall Limit.**

- High  $\beta$  duration was extended with addition of “derivative gain” in feedback loop (both for “Smart Shell” and “Mode Control” algorithms).
- Modest improvement in high  $\beta$  plasma duration is consistent with VALEN predictions of control coil (C-coil) coupling to  $n=1$  RWM.

2000: Validate Model for Active Control. Optimize Control With Six-Element C-coil.

- Validate quantitative 3-D model for  $n=1$  feedback control.
- Extend the regime of improved stability with closed-loop feedback control, with higher power using three bipolar power supplies.
- Finalize design of upgraded external coil set for improved feedback control.

2001–2002: Feedback With Upgraded C–coil

- Install upgraded C–coil set.
- Demonstrate sustained operation significantly above the no-wall beta limit in high performance AT plasmas.

**Proposed Experimental Plan for 2000**

1. Active Control of the Resistive Wall Mode (5 days)
  - Test range of leading active feedback control algorithms:
    - Optimal Smart Shell
    - Soft Rotor Stabilization
    - Mode Control Algorithm
  - Explore range of RWM target plasmas: SND and DND
  - Lower  $\delta B_r$  detection threshold for the RWM:
    - Establish required level of mode delectability
    - Use the extended saddle coil sensor array
    - Use toroidal array of  $B_p$  for  $n=1$  mode detection
2. RWM Physics Studies (2 days)
  - Effect of Plasma Rotation
  - Seed error field amplification above & below the no-wall limit
  - Effect of  $q_{\min}$  on rotation threshold
  - Effect of rational flux surfaces at plasma edge on threshold
  - Improved soft x-ray measures of mode structure
  - Use C–coil system for improved error correction for present DND AT plasmas.
3. Active Control of Locked Modes (1 day)
  - Density Limit Locked Modes
  - Quasi Stationary Modes
  - Locked NTM control

**2.4.5. Optimum Edge, Research Thrust 5 — Develop the Basis for Choosing Single- Versus Double-Null and the Optimum Triangularity of the Outermost Flux Surface in Future Machine Designs (Leader: M.E. Fenstermacher Deputies: T.H. Osborne, T.W. Petrie)**

This thrust seeks to accumulate a large body of detailed systematic measurements and analysis aimed at building a deeper understanding of the physics of the coupled regions just inside the separatrix (the H–mode pedestal region) and the region just outside the

separatrix (the SOL and divertor). In the FY99 experimental campaign this thrust implemented a set of systematic data scans to obtain detailed edge pedestal, divertor information, and other plasma performance measures versus the triangularity, the distance between the separatrices, and the volume of the divertors of a double-null. This information is expected to answer key questions of future machine design related to the best shape of the outermost flux surface, focusing on an edge physics point of view. Although the experimental portion of the thrust is complete, significant data analysis will continue in FY2000 leading to a final report and recommendations on how to revisit the question of the effect of plasma shape for an optimized advanced tokamak core with internal profile control.

### **Low Triangularity, High Density and High Confinement with Gas Fueling and Divertor Pumping (T.H. Osborne)**

In the Thrust 5 experiments focussed on triangularity, discharges with  $n_e/n_G = 1.4$ , and energy confinement enhancement over L-mode scaling,  $H_{ITER89P} = \tau_E/\tau_{ITER89P} = 1.9$  were obtained with gas puffing in combination with divertor pumping. Here  $n_G$  is the Greenwald density,  $n_G = I_p/(\pi a^2)$ . Gas puff fueling of unpumped H-mode plasmas typically leads to loss of energy confinement when the electron density,  $n_e$ , approaches the Greenwald density. Divertor pumping acts to maintain the temperature in the X-point region as high as possible while the H-mode pedestal temperature,  $T^{PED}$ , decreases and the pedestal density,  $n^{PED}$ , increases with gas puffing at roughly constant  $p^{PED}$ , in the Type I ELM regime. Maintaining high X-point temperature may avoid a transition from the Type I ELM regime to L-mode or to the Type III ELM regime in which confinement is reduced.

The high density good confinement discharges on DIII-D show spontaneous reappearing of the density profile in the Type I ELM regime which, in the highest density cases, compensates for a reduction in  $p^{PED}$ . The usual decrease in energy confinement in the Type I ELM regime with gas puffing is associated with a reduction in  $p^{PED}$  and a broadening of the density. The reduction in  $p^{PED}$  begins in the range  $0.6 < n_e^{PED}/n_G < 0.8$  and is a result of the decrease in edge pressure gradient at low temperature. The pressure gradient decrease is consistent with what would be expected for a transition from ideal to resistive tearing modes. The effect of the reduction in  $p^{PED}$  is through stiffness of the temperature profile which is apparent in the high density regime on DIII-D. The energy confinement is also reduced in discharges with stiff temperature profiles when the density profile broadens at fixed  $p^{PED}$ . The density profile peaking occurs under conditions that reduce the central temperature suggesting the neoclassical Ware pinch.

### Effect of Variation in Up/Down Magnetic Balance (T.W. Petrie)

Thrust 5 experiments also systematically varied the magnetic balance of highly triangular ( $\delta \approx 0.8$ ), unpumped H-mode plasmas. Changes in divertor heat loading and particle flux, energy confinement, and density operating range in H-mode were observed when the magnetic configuration was varied from a balanced double-null (DN) divertor to a slightly unbalanced DN divertor. To quantify “magnetic balance,” we define a parameter  $dr_{SEP}$ , which is the radial distance between the upper divertor separatrix and the lower divertor separatrix, as determined at the outboard midplane.

For attached plasmas, the variation in heat flux sharing between divertors is large for small changes in  $dr_{SEP}$  near 0 (i.e., near double-null); the peak heat flux shifts predominantly from one divertor to the other divertor within  $\pm 5$  mm of magnetic balance (Fig. 19, red curve). This sensitivity can be shown to be consistent with the measured scrape-off length of the parallel divertor heat flux,  $\lambda_q$ . Furthermore,  $\lambda_q$  can be approximated to within a factor of two with a simple model using only the midplane scrape-off lengths of electron density and temperature, suggesting that divertor processes (e.g., recycling) are not dominating the physics. At magnetic balance ( $dr_{SEP} = 0$ ), we find that the peak heat flux toward the divertor in the grad-B direction is twice that of the other divertor. Most of the heat flux goes to the outboard divertor legs in a balanced double-null, where the peak heat flux in the outer divertor may exceed that of the inner divertor by tenfold. The variation of the peak particle flux between divertors is less sensitive to changes in magnetic balance, suggesting that divertor processes are much more important here than in the heat flux case. We believe that these divertor “asymmetries” are driven by  $E \times B$  poloidal drifts. In detached plasmas, however, we find the heat flux split between divertors to be much less sensitive to  $dr_{SEP}$  (Fig. 19, green curve).

Variations in magnetic balance affect plasma performance in other ways. The density at the H-L back transition may be 15%–20% lower for an unbalanced double-null biased away from the grad-B direction, with most of this change occurring near magnetic balance. Regardless of how the divertors were magnetically balanced, however, D<sub>2</sub> gas puffing always degraded energy confinement to the range  $\tau_E/\tau_{E89L} \approx 1.3$ –1.6. When this point was reached,  $\tau_E$  stayed nearly constant, even as these plasmas were fueled to near their respective density limits

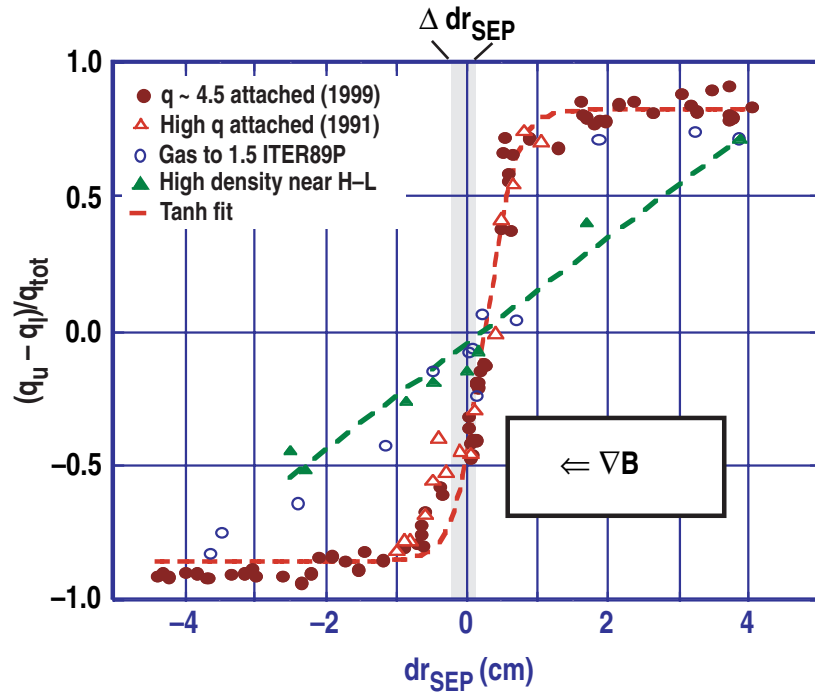


Fig. 19. Normalized peak heat flux balance as a function of magnetic balance parameter  $dr_{SEP}$ . Data from attached plasmas in the 1999 campaign at moderate  $q_{95} \sim 4.5$  (red circles) and hyperbolic tangent fit (red dashed line) show a sharp transition from lower to upper heat flux dominance as  $dr_{SEP}$  is varied from slightly unbalanced lower single-null ( $dr_{SEP} = -0.5$  cm), through balanced double-null ( $dr_{SEP} = 0$ ) to slightly unbalanced upper single-null ( $dr_{SEP} = +0.5$  cm). Uncertainty of  $dr_{SEP}$  is approximately 0.2 cm (grey bar). Data from a single swept shot in 1991 at high  $q_{95}$  (red triangles) showed a similar transition. In high density (blue open circles) and partially detached operation (green triangles) the transition is much broader indicating the importance of local recycling effects in the divertor.

### Effect of Variation in Divertor Volume (M.E. Fenstermacher)

The third subdivision of Thrust 5 attempted to address the desire to achieve the performance advantages of high triangularity (high- $\delta$ ) operation with the core plasma volume maximized and the divertor volume minimized. At low  $\delta$  in single-null divertor configurations, only the primary X-point is present inside the vacuum vessel. As  $\delta$  is increased the location of the secondary X-point, which maps at the midplane to a flux surface radially outboard of the primary, moves from outside the vacuum vessel to inside and divertor physics (recycling, target heat flux etc.) becomes important in this secondary divertor. Since the secondary divertor takes up volume that could be used for the burning core plasma, the focus of these experiments was to determine the minimum secondary divertor volume consistent with good core, pedestal and divertor performance.

The sensitivity of edge pedestal and divertor performance parameters to reduction in secondary divertor volume was examined by varying the vertical distance of the sec-

ondary X-point from the target plate,  $1 \text{ cm} < Z_s < 16 \text{ cm}$ , while holding the primary X-point height,  $Z_p = 16 \text{ cm}$ , fixed. For these discharges the ion  $\nabla B$  drift was in the direction of the primary divertor. Discharges with and without active primary divertor cryopumping were examined. The effective rate of rise of the core density at the L-H transition increased 60% as  $Z_s$  was reduced from 16 to 1 cm. At high density achieved by gas injection, the core line averaged density at the H-L back transition decreased 25% as  $Z_s$  was reduced. Both of these results indicate that performance may be affected when core plasma screening of neutrals in the secondary divertor is reduced as  $Z_s$  decreases. The peak heat flux in the secondary divertor ( $P_{\text{div}}^s$ ) was nearly constant for high  $Z_s$ . However, when  $Z_s$  was reduced from 3 cm to 1 cm,  $P_{\text{div}}^s$  increased a factor of 3 indicating that the secondary divertor target was beginning to act as a heat flux limiter as  $Z_s$  became comparable to the power scale length in the scrape-off-layer mapped to the secondary X-point location. Finally, for unpumped discharges the dependence of the maximum achieved edge pedestal temperature and pressure during the ELM-free period was nonlinear with  $Z_s$ . The dependence on  $Z_s$  was very weak for discharges with active pumping. Boundaries between Type-I ELMing and Type-III ELMing regimes in edge pedestal operating space also seemed to depend weakly on  $Z_s$  for unpumped plasmas. Although we attempted to hold as many control parameters fixed as possible, data showed that variation in wall conditions may also have affected the edge and divertor performance somewhat. Core transport and SOL/divertor fluid simulations are in progress to identify the mechanisms connecting secondary divertor volume variation to changes in performance.

#### 2.4.6. High $\ell_i$ , Thrust 6

Work deferred until 2002. See end of Section 2.3 for the plan.

#### 2.4.7. ITB, Research Thrust 7 — Expand the Spatial Extent and Time Duration of Internal Transport Barriers (Leader: C.M. Greenfield; Deputies: E.J. Synakowski, E.J. Doyle)

##### Goals

Control of internal transport barriers (ITB) has been identified as a high priority at the recent AT Workshop held at General Atomics as well as at the Snowmass meeting. Specifically, control of three different aspects of the ITB is needed in order to establish it as a viable confinement regime.

First, the spatial extent of the barrier must be extended in order to increase the energy content and the fusion output from within the barrier region (Fig. 20). The requirement that this be done in a manner consistent with MHD stability leads to a second area of control: the pressure gradient in the barrier itself must be maintained at a level below

MHD stability limits. Third, in order to maintain a steady barrier, the current profile must be maintained so that  $q_{\min}$  remains elevated, with weak or negative shear in the core.

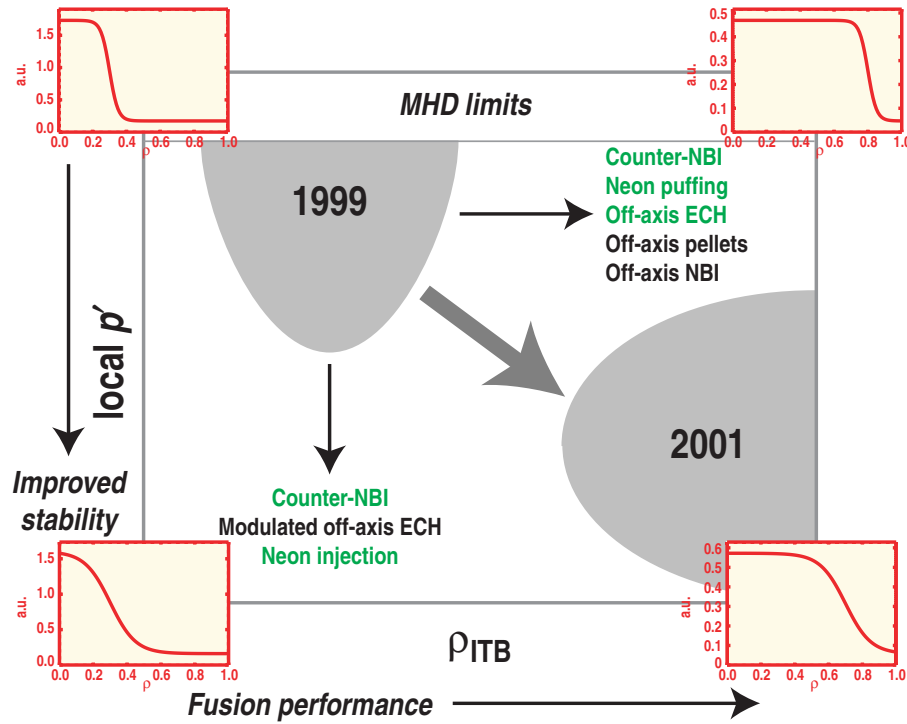


Fig. 20. Efforts in Thrust 7 are focused toward increasing fusion performance by expanding the transport barrier, while at the same time controlling the pressure gradient within the transport barrier to maintain MHD stability.

The plan for the 2000 campaign directly addresses open-loop tests of control of the first two of these requirements, with the third being addressed indirectly. Since the current three day plan does not allow for testing all of the proposed methods, the entire set of proposed open-loop tests will require two or more years. Successful completion of the proposed near-term program can lead to future closed-loop tests of ITB control with feedback.

A fourth requirement, relating to reactor relevance of the ITB regime (barring advances allowing a hot-ion mode in a reactor) is to extend the operating space toward  $T_e/T_i \sim 1$ . An experiment to explore a possible avenue toward this state is not included in the five day plan, but is included as a possible contingency experiment.



## 1999 Progress

Experiments in 1999 concentrated on studies of the ITB with counter-injected neutral beams. As might be expected with any new regime, development of the regime took most of the time allocated, with only a small amount of time left for actual optimization of study. Nevertheless, the experiments were successful in demonstrating that barriers can be formed with counter-NBI, and are broader than their co-injected counterparts. This is not surprising, since with co-injection, the diamagnetic and toroidal rotation terms of the  $E \times B$  shearing rate oppose in such a way that broadening or increasing the pressure gradient will *decrease* the shearing rate, thereby allowing drift ballooning modes such as the ITG mode to become more unstable. With counter-NBI, the two terms are aligned so that increasing or broadening the pressure profile can actually be stabilizing to such microinstabilities [C.M. Greenfield, *et al.*, GA-A23305, submitted to Phys. Plasmas] (Fig. 21). Although progress was made in exploiting this feature of counter-NBI, it is believed that further optimization with counter-injection may allow further ITB broadening.

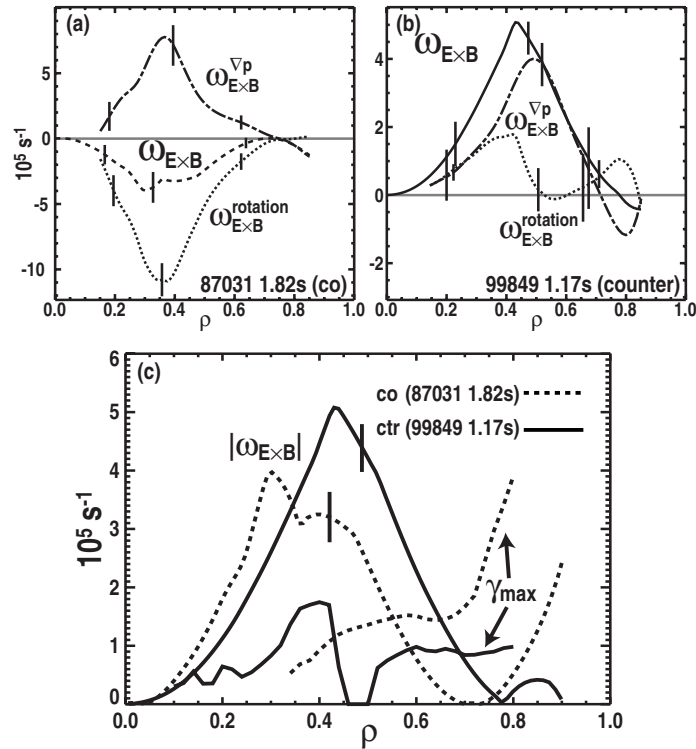


Fig. 21. Main ion pressure gradient and rotation terms of the  $E \times B$  shearing rate are opposed with co-, and aligned with counter-injection so that increasing or broadening the pressure profile is stabilizing to drift-ballooning modes with counter-injection.

Another important feature of counter-injection is that counter-neutral beam current drive (NBCD) was successful in arresting the evolution of the current profile during the ITB phases of the discharge. With finer control of the neutral beam power, we believe there is a possibility of simultaneously exploiting both the favorable effect on the shearing rate and the counter-NBCD to expand and sustain the barrier.

First attempts at producing a transport barrier using high-field-side pellet-injection were also successful during the Thrust 7 experiments in 1999 [L.R. Baylor, *et al.*, submitted to Phys. Plasmas]. In these experiments, extremely steep barriers were produced in the electron density profile, with  $T_e/T_i \sim 1.25$  achieved and maintained for hundreds of ms with counter-injection.

Although not carried out within Thrust 7, DIII-D demonstrated that impurity injection can produce transport barriers by decreasing the ITB growth rates [G.R. McKee, *et al.*, submitted to Phys. Plasmas]. This tool will be incorporated into our efforts within Thrust 7.

Finally, an experiment was carried out to determine the relationship between the transport barrier location and the location of the minimum safety factor  $\rho_{qmin}$  [M. Makowski, Bull. Am. Phys. Soc. **44**, 77 (1999). Paper CP1 87]. Incorporating a fast current ramp and high power neutral beam (co) injection very early in the discharge did this. Although discharges were produced with very large  $\rho_{qmin} \leq 0.9$ , the transport barrier was not formed at this large radius. It is felt that the aforementioned cancellation of terms of the shearing rate may be responsible for limiting the barrier location in such co-injected discharges. Although a proposal was made to follow this up with a similar experiment in a counter-injected plasma, it has not been included on the list of experiments for 2000 due to concerns that the beam ion confinement may be too poor when combining the large orbits produced with counter-injection and the very low poloidal field inherent to these plasmas.

### **Experiments Proposed for 2000 and Beyond:**

In the year 2000, we proposed to continue development of barrier control tools, justified either by previous experiment or theoretical predictions, in an open-loop fashion. If one or more of these tools is extremely successful in modifying the barrier in the desired manner, we might choose to make an earlier transition to application in a closed-loop. Otherwise, the first phase of experiments (which will probably take 2 years or more depending on time allocations) will include open-loop tests of the following. Note that

many of these tests are intended to be performed with barriers formed by both neutral beams alone and those with pellet triggers, in order to produce two very different data points:

1. **Continued Optimization of the Counter-Injected ITB.** Attempts have been made to use fine control of neutral beam power to control the barrier position in the past, but have not been successful. We now believe that this might have been at least partially due to the cancellation of the diamagnetic and rotation terms of the shearing rate, as previously mentioned, with co-injection. In those discharges, increasing the power would result in a steepened pressure gradient and eventually to an MHD event (which could lead to either disruption or an H-mode transition). We believe that similar efforts with a counter-injected target plasma should lead to broadening of the barrier through the mechanism described in the previous section.

Further success in this area may motivate future consideration of modifying the neutral beam geometry in DIII-D by reversing the orientation of one of the beamlines.

The plasmas produced by this optimization are expected to have broader barriers and be easier to sustain than we can achieve with co-injection, and so are proposed to be used as a target condition for several of the other areas listed below.

2. **Optimization of Impurity Injection.** Previous experiments with impurities, primarily neon, have demonstrated the production of an internal transport barrier at rather limited parameters. Experiments in the next phase of Thrust 7 will attempt to extend this improvement to barriers with similar local performance to those produced with high power neutral beams alone and exhibiting higher temperatures, densities, etc. Successful application of this technique should lead to broader barriers due to the favorable influence of the impurities on microinstability growth rates in the part of the plasma where they are usually expected to be largest.
3. **Off-Axis ECH.** ECH heating (radial launch) near the axis of beam-heated discharges has previously been shown to result in deterioration of the transport barrier [C.M. Greenfield, *et al.*, Nucl. Fusion **39**, 1723 (1999)]. Theoretical predictions [G.M. Staebler, *et al.*, EPS 1998] have been made which indicate that the same effect can be used in our favor, by injecting ECH outside the ITB, thereby causing the ITB to move toward the heating location. Further predictions [D. Newman, private communication (1999)] indicate that modulated ECH injected in two locations, just inside and outside the barrier, may be a useful tool to

control the pressure gradient in the barrier. Tests of control of both the ITB position and strength are proposed using off-axis ECH in both ways. Future experiments may even be able to do both of these simultaneously.

4. **Off-Axis Pellet Injection.** Utilization of shallow pellet injection, just outside the barrier, may be another means of expanding the barrier in a similar manner as with off-axis ECH. The primary mechanism here is expected to be in the angular momentum, rather than a thermal, transport channel.
5. **Magnetic Braking.** Magnetic braking may be used to remove momentum to simulate the case where balanced injection is used to maintain broader barriers, as in JT-60U [H. Shirai, *et al.*, H-mode Workshop 1999]. Although using field errors to brake the plasma may not ultimately be a desirable situation, this may also help to motivate future changes to beam geometry.
6. **Off-Axis NBI.** Shifting the plasma above the midplane of the tokamak can be used to move the neutral beam heating location significantly off-axis. This is expected both theoretically and experimentally to result in a broader barrier. Once again, this may not lead to an attractive scenario in DIII-D as it is presently configured, but may be used to motivate future considerations of modifications to the neutral beam geometry.

One other experiment is proposed for inclusion in this phase of the experimental program. Recently, ASDEX-U incorporated counter-ECCD in a beam-heated discharge to produce an internal transport barrier with  $T_e(0) \approx T_i(0) \approx 12$  keV [F. Leuterer, *et al.*, EPS 1999; O. Gruber, *et al.*, H-Mode Workshop 1999; R. Wolf, *et al.*, submitted to Phys. Plasmas]. This regime is a challenge to our understanding and previous experience with the impact of electron heating in ITB discharges. However, if it can be duplicated, this regime offers perhaps a more reactor-relevant scenario than the hot-ion modes usually produced with an ITB. We propose to attempt to produce plasma in this regime both to demonstrate the regime itself and in an attempt to understand the underlying physics and how it differs with our previous experience.

Future experiments, nominally planned for the third year of this plan, will incorporate the most promising results of these closed-loop tests in a demonstration of a controlled barrier utilizing feedback control of one or more of these tools.

### 3. TOPICAL SCIENCE AREAS — THREE YEAR VIEWS

#### 3.1. STABILITY TOPICAL AREA GOALS (3 YEAR VIEW)

1. Advance the physics understanding of resistive wall mode stability, including the dependence on plasma rotation, wall distance, and feedback stabilization.  
*Develop sustained operation above the no-wall beta limit through passive or active stabilization of the resistive wall mode.*
2. Characterize the physics of edge-driven instabilities in plasmas with a large (H-mode) edge pressure gradient and associated bootstrap current.  
*Develop methods to avoid or reduce the impact of edge-driven instabilities through modification of the edge pressure gradient, collisionality, or shaping.*
3. Advance the physics understanding of non-ideal plasma instabilities including neoclassically driven tearing modes, sawteeth, and fast ion driven instabilities.  
*Develop sustained high beta operation free of sawteeth and neoclassical tearing modes, through profile control or active stabilization.*
4. Advance the understanding of disruption physics in advanced tokamak discharges and improve the viability of tokamak reactor concepts by avoiding and mitigating disruptions.  
*Develop methods of mitigating runaway electron, halo currents, and disruption heat loads, and disruption prediction and avoidance using real-time identification of disruption boundaries.*

#### 3.2. CONFINEMENT AND TRANSPORT TOPICAL AREA GOALS (3 YEAR VIEW)

Physics research aims at a level of understanding that allows quantitative predictions. In the transport arena in magnetic fusion research, this means the development of a predictive understanding of the energy, particle and momentum transport in magnetized plasmas. Achieving this goals requires the combined efforts of theorists, modelers and experimentalists to develop the fundamental theories, include them in numerical models,

compare those models with the results of experiments and then iteratively improve them. Based on this ultimate goal, our three year goals for confinement and transport are:

1. Develop improved physics understanding and control of reduced core transport regions
  - Develop and exploit new tools for controlling core transport: Pellet injection, impurity injection, counter neutral beam injection, co and counter ECCD.
  - Broaden tests of the  $\omega_{\text{EXB}}$  versus  $\gamma_{\text{MAX}}$  comparison by using new tools to investigate effect of  $T_i/T_e$  ratio, impurities, density peaking, magnetic shear.
  - Increase emphasis on understanding electron transport.
2. Investigate fundamental nature of turbulent transport in tokamaks.
  - Is complex dynamics (avalanches) a better fundamental model than a theory in which fluxes depend continuously and smoothly on gradients?
  - Can we identify features in the data which are unique to the fundamental theoretical microturbulence modes (e.g. ITG, ETG, TEM)?
  - Compare measured turbulence characteristics with gyrokinetic and gyrofluid code predictions.
3. Carry out innovative experiments to make quantitative tests of predictions of (theory-based) transport models
4. Utilize nondimensional scaling approach to further elucidate tokamak transport
  - Use this approach to define an attractive next-step device based on ELMing H-mode.
5. Test theories of edge and divertor conditions needed to get H-mode
  - Quantitatively test the new set of analytic theories developed in Europe.
  - Encourage detailed comparison of US numerical work (e.g. Drake, Xu) with experimental results.
  - Determine if plasma parameters alone govern threshold or whether atomic physics (e.g. neutrals) is also important.
6. Investigate fundamental nature of L to H transition.
  - Physics of pellet triggered H-modes.
  - Effect of electron versus ion heat flux on transition.
  - Effect of current ramp on transition.
7. Study H-mode edge pedestal and investigate key physics controlling edge gradient and pedestal values.
8. Continue development of modeling capability in parallel with experimental tests.

## Summary of 1999 Experimental Results in the Confinement and Transport Topical Area

Although lack of ECH reduced the number of experimental days devoted to this topical science area, significant experimental results were obtained in each of the five experimental days devoted to it in 1999. Perhaps the most impressive set of results were obtained in the experiment that investigated use of impurity injection to improve the core confinement (RI-mode). As was reported in G.R. McKee's invited talk at the APS DPP meeting in Seattle, neon, argon and krypton injection were used as part of this work with neon giving the best results. The impurity injection resulted in a substantial improvement in global confinement and in the local electron and ion thermal diffusivities with the ion improvement being the greater. The reduction in transport was clearly correlated with reduced density fluctuations as measured by beam emission spectroscopy and by far infra-red scattering. Comparisons between the  $E \times B$  shearing rate and the gyrokinetically-determined turbulence growth rate showed that the  $E \times B$  shearing rate was below the growth rate before impurity injection but exceeded it after injection. In other words, impurity injection reduced the turbulence growth rate so that the  $E \times B$  shear feedback loop could result in reduced transport. Preliminary evidence was obtained of a change in the high- $\kappa$  ( $\kappa \sim 13 \text{ cm}^{-1}$ ) fluctuations which correlated with the confinement improvement, suggesting that impurity effects on short wavelength fluctuations may be connected with the reduction in electron thermal transport. In addition to providing a wealth of fundamental physics, this experiment has given us a new tool for triggering core transport reduction.

In the H-mode physics area, we combined several experiments into one set of shots in order to maximize the amount of information that we could obtain. Two results from this day stand out. First, we used the beam emission spectroscopy system to obtain two dimensional turbulence data at the plasma edge across the L to H transition. Processing this data to produce a movie allows one to see the turbulent eddies convect past the field of view. These results were presented in R. Fonck's invited talk at the APS DPP meeting in Seattle. Second, we thoroughly documented the pellet-triggered H-modes which we had first identified on DIII-D in 1998. Both high and low field side launch pellets can trigger the H-mode with the power threshold reduction being greater for the high field side launch. The best result was a reduction in power threshold by about 2.5 MW (30%).

In addition to the planned experiments, we made a serendipitous discovery this year of a mode of operation with no ELMs and no sawtooth oscillation which had controlled, constant density and impurity levels. These discharges were created using counter neutral beam injection to plasmas where the density was lowered using cryopumping. The operational key was a line averaged density below  $\lesssim 3 \times 10^{19} \text{ m}^{-3}$  and a neutral beam power above about 7.5 MW. The constant density and impurity levels are connected with the

presence of low level MHD oscillations in the plasma edge which apparently increase the particle transport enough that cryopumping is still effective in spite of the absence of ELMs. These oscillations have little effect on the H-mode edge pressure profiles; the profile width is the same whether or not these modes are present. A key issue for divertor design for a fusion reactor is the pulsed heat load to the divertor plates caused by ELMs. The ELM-free operation seen in these discharges solves these problems by getting rid of the ELMs without paying the usual price of uncontrolled density rise in an ELM-free phase. If we can understand why this occurs and apply this in reactor plasmas, we will have solved a significant problem in fusion reactor design.

The Fundamental Turbulence Studies group performed an experiment whose primary goal was to provide a comprehensive test of whether ion temperature gradient (ITG) turbulence is the dominant microinstability and source of anomalous transport in DIII-D as predicted by theory. The experiment was performed by study the changes in turbulence during a density scan in Ohmic plasmas from the neoAlcator regime and into the saturated Ohmic confinement regime. Far infra red scattering measurements did see an enhanced low frequency feature in the scattered spectra at high density, consistent with the theoretical prediction that the ITG mode is more unstable there. Theory also predicts that the electron temperature gradient mode (ETG) is important at all densities; reflectometry measurements indicate the presence of two modes. More detailed comparisons with the predictions of gyrokinetic codes is in progress.

In 1999, nondimensional transport studies concentrated on the effect of rotation on confinement using counter neutral beam injection. A previous, co-injected  $\rho_*$  scan in ELMing H-mode plasmas was duplicated with all the dimensional parameters except the Mach number and  $Z_{\text{eff}}$ . The  $\rho_*$  scaling of global confinement was Bohm-like for counter injected discharges while the one for co-injected discharges was gyroBohm-like. Theory-based transport modeling is now needed to see if this change in the transport scaling can be explained either by the different Mach number and, hence, different  $E \times B$  shearing rate or by the differing  $Z_{\text{eff}}$ .

In the area of core transport barrier physics and control, we investigated whether ICRF could be used to control the plasma toroidal rotation. Theoretical predictions indicate that spatial transport of resonantly heated ions could produce torques on the plasma which might alter the toroidal rotation. Previous DIII-D experiments in had also shown that electron heating from ICRF fast wave and ECH increased radial transport of angular momentum, also altering toroidal rotation. The goal of the experiment was to see which of these effects is dominant in our plasma. By utilizing counter neutral beam injected plasmas, we set up a condition where the postulated ICRF torque would increase the magnitude of the rotation while the electron heating effect would decrease it. The results were consistent with the increased transport being the dominant effect.



### 3.3. DIVERTOR/EDGE PHYSICS TOPICAL AREA GOALS (3 YEAR VIEW)

The main function of the boundary plasma is to control particle and power flux at the interface between the core plasma and the material walls. The long range goal of the DIII-D divertor and scrape-off layer science program is to: (1) use state-of-the art 2-D diagnostics to identify the relevant physical processes, (2) model these processes with computational models (e.g. UEDGE), and (3) sufficiently understand the relevant physical processes in the edge plasma so that computational models can predict operation for new operating modes on existing machines and for new machine designs.

We have identified and studied the radiative divertor or “detached” mode of operation which reduces the heat and particle flux in the divertor by deuterium puffing. Intrinsic carbon radiation is a key ingredient in this mode. We plan to extend the operating regime (i.e., operation at lower core  $n_e$ ) for near-term AT operation by concentrating radiation in the divertor with injected impurities such as argon. The two tools to achieve this goal are so-called “puff and pump” techniques, (deuterium injection and pumping to provide a force on impurities towards the divertor) and divertor baffling (to better control neutrals). The baffling and pumping are also important ingredients in the control of density and impurities for the core plasma. We will also investigate the role of triangularity, single-null, and double-null on both divertor and AT conditions. Substantial progress has been made in the measurement (DiMES probe) and modeling (REDEP) of erosion and redeposition in the DIII-D divertor during detached operation. These studies will be continued during the next phase of impurity radiative divertor operation. They are also important in understanding the best means to control carbon radiation in an all-carbon machine like DIII-D.

#### 3.3.1. 1999 Divertor/Edge Progress

The experiments in the Edge and Divertor area were executed both in the Divertor Topical Science area and Thrust 5; the latter work was focused on the effects of plasma shape in unbalanced double null plasmas. The experiments that were specifically done in the divertor area focused on plasma flows and carbon sources and transport. We obtained new flow data with both the Mach probes and the spectroscopic diagnostic in detached plasmas. Measurements with divertor biasing in ohmic plasmas showed that the divertor potential could be changed with biasing. DiMES measurements (DiMES is an impurity probe) showed that there was no appreciable net erosion in detached plasmas. Data also indicated that the net carbon source in DIII-D has been decreasing over the past seven years (presumably due to wall condition of the graphite), but the core carbon concentration has not changed appreciably. Carbon sources and transport will also be an important topic in the FY2000 campaign. Experiments at high core electron density (greater than the Greenwald density) were performed; degradation of confinement was

not observed. We are now theorizing that divertor pumping may play an important role in this operation, and will be the focus of one run day in FY 2000.

### **3.3.2. 2000–2001 Work**

At the start of the year 2000 we will have several new boundary research tools at our disposal which will significantly enhance our ability to conduct experiments in support of the DIII-D Advanced Tokamak and Boundary Physics program goals. The private flux cryopump-baffle system will be commissioned. The graphite armor tiles in the vicinity of the new divertor system will be improved so that they follow the field lines more closely, thereby reducing the number of sharp edges that can overheat. The new capabilities apply to single-null and biased double-null configurations while allowing a side by side comparison of the closed and open configurations.

With these modifications we will have the capability of independently pumping both legs of the divertor, reducing the core neutral source in single-null by an estimated factor of six relative to an open configuration, and sustaining AT plasmas up to the device volt-second limit before reaching the tile thermal limit. New research made possible by these modifications include:

1. Impurity control by the forced flow technique (“puff and pump”) may be extended to lower density plasmas, and perhaps even to ELM-free plasmas. If successful, the technique will be used routinely to reduce carbon concentration in AT plasmas.
2. Research to expand the volume of radiative zone by convection.
3. Study feasibility of stable fully detached plasmas.
4. Investigate stability and confinement of density controlled rectangular cross-section plasmas.
5. Isolate the effect of neutrals on edge transport barrier and L-H transition.
6. Investigate heat flux control at densities compatible with AT scenarios using a combination of mantle and divertor radiation and application of convection.

The first order of business in the year 2000 is to evaluate the new system for these applications. The actual detailed experiments will be spread out through years 2000–2002. The commissioning work includes; evaluation of the result of improved wall armor on carbon content of the plasma, optimization and control of pumping configurations, preliminary evaluation of impurity reduction by bi-directional forced flow, and neutral density decrease due to the new baffle system. These preliminary rough measurements

will be followed by more detailed focused experiments in years 2001 and 2002 as described below.

### **3.3.3. Details of the Year 2000 and 2001 Experiments**

1. Determine conditions necessary for divertor impurity enrichment. Make extensive use of the full upper RDP.
2. Develop radiative mantle discharges.
3. Develop heat flux reduction techniques at AT-like edge conditions.
4. Determine steps required to minimize carbon influx in high performance plasmas.
5. Demonstrate predictive capability of erosion/redeposition pattern in the DIII-D tokamak.

### **3.3.4. 2002 Work**

1. Continue to develop radiative divertor and mantle solutions compatible with the density operation needed for the (near-term) AT core plasma scenarios.
2. Attempt an integrated divertor/core demonstration as an element of the NCS scenario work.
3. Prove viability of poloidal tokamak divertor concept by demonstrating control of erosion and co-deposition.

The outcome of the years 2001 and 2002 AT and divertor experiments will guide us towards the future course of the divertor effort. The options in the near future are:

1. Accept the single-null/biased double-null configuration, perhaps with a number of refinements such as an inner wall bump to increase the amount of baffling (but limit the shape flexibility).
2. Proceed to a full double-null divertor configuration.

## **3.4. HEATING AND CURRENT DRIVE TOPICAL AREA GOALS (3 YEAR VIEW)**

1. Establish predictive capability for ECCD, including dependencies on density, temperature,  $Z_{\text{eff}}$ , geometry, power, trapping, and dc electric field.
2. Advance the physics understanding of FWCD, including effects of frequency,  $n_{\parallel}$ , competing edge losses, high harmonic absorption on beam ions and thermal ions, rf-

induced resonant ion transport, wave propagation, conservation of toroidal mode number.

3. Advance the understanding of NBCD, including the effects of fast particle modes and TAE modes. This would involve development of a model of fast ion transport.
4. Understand the effects of heating of electrons and/or ions on plasma rotation and transport, particularly transport barriers.
5. Develop long pulse discharges with full noninductive current drive, including discharges with very high bootstrap fraction as a step toward transformerless operation.
6. Develop routine electron heating using the ICRF system, through fast wave and/or second harmonic hydrogen minority heating (especially at high density where beam penetration is poor). Develop minority heating for sawtooth stabilization and minority or beam ion current drive.